

Effects of *Melandrium firmum* Rohrbach on RANKL-induced osteoclast differentiation and OVX rats

MINSUN KIM, JAE-HYUN KIM, SOOYEON HONG, BOGUEN KWON,
EUN-YOUNG KIM, HYUK-SANG JUNG and YOUNGJOO SOHN

Department of Anatomy, College of Korean Medicine, Kyung Hee University, Seoul 02447, Republic of Korea

Received December 10, 2020; Accepted April 26, 2021

DOI: 10.3892/mmr.2021.12248

Abstract. Osteoporosis is a systemic skeletal disease characterized by reduced bone mineral density (BMD), which results in an increased risk of fracture. *Melandrium firmum* (Siebold & Zucc.) Rohrbach (MFR), ‘Wangbulryuhaeng’ in Korean, is the dried aerial portion of *Melandrii Herba* Rohrbach, which is a member of the Caryophyllaceae family and has been used to treat several gynecological conditions as a traditional medicine. However, to the best of our knowledge, the effect of MFR on osteoclast differentiation and osteoporosis has not been assessed. To evaluate the effects of MFR on osteoclast differentiation, tartrate-resistant acid phosphatase staining, actin ring formation and bone resorption assays were used. Additionally, receptor activator of nuclear factor- κ B ligand-induced expression of nuclear factor of activated T cell, cytoplasmic 1 (NFATc1) and c-Fos were measured using western blotting and reverse transcription-PCR. The expression levels of osteoclast-related genes were also examined. To further investigate the anti-osteoporotic effects of MFR *in vivo*, an ovariectomized (OVX) rat model of menopausal osteoporosis was established. Subsequently, the femoral head was scanned using micro-computed tomography. The results revealed that MFR suppressed osteoclast differentiation, formation and function. Specifically, MFR reduced the expression levels of osteoclast-related genes by downregulating transcription factors, such as NFATc1 and c-Fos. Consistent with the *in vitro* results, administration of MFR water extract to OVX rats reduced BMD loss, and reduced the expression levels of NFATc1 and cathepsin K in the femoral head. In conclusion, MFR may contribute to alleviate osteoporosis-like symptoms. These results suggested that MFR may exhibit

potential for the prevention and treatment of postmenopausal osteoporosis.

Introduction

Osteoporosis is a systemic skeletal disease characterized by reduced bone density, which leads to an increased risk of fracture (1). Osteoporosis is considered a public health problem, the prevalence of which is increasing worldwide (2). Bone homeostasis requires maintenance of a balance between osteoclast-induced bone resorption and osteoblast-induced bone formation; however, an increase in osteoclast number and activity can result in an imbalance in bone remodeling (3). This imbalance can result in osteoclast-mediated bone diseases, such as rheumatoid arthritis, periodontal disease, Paget's disease and osteoporosis (4).

Bisphosphonate and hormone replacement therapy with estrogen are the most widely used treatments for postmenopausal osteoporosis (5). However, long-term treatment with bisphosphonate is unsuitable for several patients with osteoporosis owing to serious side effects, such as osteonecrosis of the jaw, atrial fibrillation, esophageal cancer, musculoskeletal pain and atypical fractures (6-9). In addition, hormone replacement therapy has unwanted side effects, such as an increased risk of developing ovarian cancer and breast cancer (10-12). Thus, it is essential to discover novel effective and safe treatments for osteoporosis.

Osteoclasts are multinucleated giant cells derived from monocyte/macrophage hematopoietic precursor cells (13). Receptor activator of nuclear factor (NF)- κ B (RANK) ligand (RANKL) is an essential cytokine of osteoclast differentiation (14). Binding of RANKL to RANK induces recruitment of the adaptor protein tumor necrosis factor (TNF) receptor-associated factor (TRAF6). TRAF6 induces the translocation of NF- κ B (15,16). These signaling pathways are responsible for the activation of key transcription factors, such as c-Fos and nuclear factor of activated T cell, cytoplasmic 1 (NFATc1), resulting in increased expression of osteoclast-specific genes, including tartrate-resistant acid phosphatase (TRAP/*Acp5*), ATPase H⁺ transporting V0 subunit D2 (*ATP6v0d2/Atp6v0d2*), osteoclast-associated immunoglobulin-like receptor (OSCAR/*Oscar*), cathepsin K (CTK/*Ctsk*) and matrix metalloproteinase-9 (MMP-9/*Mmp9*) (17-20).

Correspondence to: Professor Youngjoo Sohn, Department of Anatomy, College of Korean Medicine, Kyung Hee University, 26-6 Kyungheedaero, Dongdaemun-gu, Seoul 02447, Republic of Korea
E-mail: youngjoos@khu.ac.kr

Key words: *Melandrium firmum* Rohrbach, osteoclasts, receptor activator of nuclear factor- κ B ligand, nuclear factor of activated T cell, cytoplasmic 1, c-Fos, ovariectomized rats

Melandrium firmum (Siebold & Zucc.) Rohrbach (MFR) is the dried aerial portion of *Melandrii Herba Rohrbach*, a member of the Caryophyllaceae family. MFR is known as 'Wangbulryuhaeng' in Korea and has been traditionally used to treat gynecological conditions, such as breast cancer and lactation disorders (21). Previous studies have shown that the methanol extract of MFR exhibits an anti-inflammatory effect on lipopolysaccharide (LPS)-induced proinflammatory cytokines, such as TNF- α and interleukin (IL)-1 β (22,23). According to previous studies, inhibition of TNF- α and IL-1 β has been associated with metabolic bone disease, such as postmenopausal osteoporosis and rheumatoid arthritis. IL-1 β has been revealed to be regulated by RANKL to increase activity and promote osteoclast formation (24,25). In addition, TNF- α may serve an important role in regulating bone homeostasis by stimulating osteoclast formation and inhibiting osteoblast function (26,27). Furthermore, vitexin, another active compound found in MFR, has been shown to inhibit osteoclastogenesis and prevent LPS-induced osteolysis (28). Based on these previous findings, it was hypothesized that MFR may potentially attenuate osteoclast differentiation, thus preventing bone loss in osteoporosis. However, to the best of our knowledge, the effect of MFR on osteoclast differentiation and osteoporosis is yet to be explained.

In the present study, the effect of MFR on osteoclast differentiation in RANKL-induced mouse macrophage RAW 264.7 cells and bone loss in an ovariectomized (OVX) rat model of osteoporosis was assessed.

Materials and methods

Reagents. DMEM was purchased from Welgene, Inc. Minimum essential medium- α (α -MEM), penicillin/streptomycin (P/S) and Dulbecco's PBS (DPBS) were obtained from Gibco; Thermo Fisher Scientific, Inc. FBS was purchased from Atlas Biologicals. RANKL was purchased from PeproTech, Inc. CellTiter 96 Aqueous non-radioactive cell proliferation (MTS) assay was purchased from Promega Corporation. Bicinchoninic acid (BCA) solution, phosphatase inhibitor cocktail, DAPI, 17 β -estradiol (E₂) and alendronate (ALN) were obtained from Sigma-Aldrich; Merck KGaA. Osteo Assay Surface multiple well plates (cat. no. 3989) were obtained from Corning, Inc.. PCR primers were synthesized by Genotech Corp. Acti-stain™ 488 Fluorescent Phalloidin was purchased from Cytoskeleton, Inc.. The primary antibodies and secondary antibodies used in the present study were: β -actin (cat. no. sc-8432; Santa Cruz Biotechnology, Inc.), c-Fos (cat. no. sc-447; Santa Cruz Biotechnology, Inc.), NFATc1 (cat. no. 556602; BD Biosciences), MMP-9 (cat. no. ab38898; Abcam), CTK (cat. no. ab19027; Abcam), TRAF6 (cat. no. sc-8409; Santa Cruz Biotechnology, Inc.) and peroxidase AffiniPure Goat Anti-Mouse IgG (cat no. 115-035-062; Jackson ImmunoResearch Laboratories, Inc.) and peroxidase AffiniPure Goat Anti-Rabbit IgG (cat no. 115-035-144; Jackson ImmunoResearch Laboratories, Inc.). All other reagents used were of analytical grade.

Preparation of MFR extract. MFR was purchased from Omniherb. MFR was prepared by decocting 300 g of the dried herb in 1.5 l boiling distilled water (D.W) for 2 h. The

extract was filtered using filter paper (no. 3; Whatman plc; GE Healthcare Life Sciences) and collected in a rotary evaporator at 55°C. The extract was lyophilized and 19 g dried powder was obtained (yield ratio, 12.7%).

High-performance liquid chromatography (HPLC) analysis. Vitexin (cat. no. 49513; Sigma-Aldrich; Merck KGaA) is the active ingredient in MFR (29); therefore, to quantitatively evaluate the MFR extract, HPLC was performed with vitexin used as an internal standard. Vitexin was prepared in DMSO. Analysis was performed using a UV detector (2996 Waters 2695; Waters Corporation); separation was carried out on an Xbridge-C18 with a C18 guard column (250 x 4.6 mm; 5 μ m; Waters Corporation) and proceeded at 30°C for 50 min at a flow rate of 1 ml/min. Vitexin was detected at 335 nm. Samples were injected in a volume of 10 μ l. The mobile phase consisted of acetonitrile (A) and water (B), at a composition of 10% A from 0-10 min and 50% A from 10-30 min.

RAW 264.7 cell culture and cytotoxicity assay. RAW 264.7 cells are mouse monocyte-macrophage like cells (30). RAW 264.7 cells were obtained from Korean Cell Line Bank; Korean Cell Line Research Foundation. RAW 264.7 cells were cultured in DMEM supplemented with 10% FBS and 1% P/S in a cell incubator at 37°C and 5% CO₂. To examine cell viability, the cells were seeded in a 96-well plate at 5x10³ cells/well and incubated for 24 h. RAW 264.7 cells were treated with MFR (12.5, 25, 50 and 100 μ g/ml) at 37°C for 24 h. After treatment, 20 μ l/well MTS solution was added and the cells were incubated at 37°C for 2 h. To determine cell viability of mature osteoclasts, RAW 264.7 cells were seeded in a 96-well plate at 5x10³ cells/well and were treated with or without RANKL (100 ng/ml) for 5 days. Subsequently, cells were treated with MFR (12.5, 25, 50 and 100 μ g/ml) for 1 day, after which, 20 μ l MTS solution was added and incubated at 37°C for 2 h. Cell viability was measured using an enzyme-linked immunosorbent assay (ELISA) reader at a wavelength of 490 nm.

TRAP staining and measurement of TRAP levels. A total of 5x10³ RAW 264.7 cells/well were seeded in a 96-well plate. After 24 h, to induce osteoclast differentiation of RAW 264.7 cells, cells were treated with RANKL (100 ng/ml) and MFR (12.5, 25, 50 and 100 μ g/ml) at 37°C for 5 days. The medium was replaced every 2 days. In order to compare the inhibitory effect of MFR and vitexin on osteoclast differentiation, cells were seeded in the same manner as mentioned previously. After 24 h, the medium was replaced with RANKL (100 ng/ml) and MFR (50 and 100 μ g/ml) or vitexin (0.0753 and 0.147 μ g/ml) at 37°C for 5 days. Subsequently, the cells were washed and fixed with 4% formalin at room temperature for 10 min. TRAP staining was performed using a TRAP kit (Sigma-Aldrich; Merck KGaA) according to the manufacturer's protocol. The number of TRAP-positive cells was counted using an inverted light microscope (Olympus Corporation; magnification, x100).

TRAP is secreted in large quantities by osteoclasts and TRAP levels are considered a biochemical marker of osteoclast function (31). Therefore, the present study also analyzed TRAP levels to determine the effect of MFR on osteoclast function. In order to measure the TRAP levels,

50 μ l differentiation medium was obtained and transferred to a new plate. Subsequently, an equal volume of TRAP solution (4.93 mg 4-Nitrophenyl phosphate disodium salt hexahydrate in 850 μ l 0.5 M acetate solution and 150 μ l tartrate solution) was added to the differentiation medium and incubated at 37°C for 1 h. Subsequently, the reaction was terminated using 0.5 M NaOH and TRAP levels were measured using an ELISA reader at a wavelength of 405 nm.

Filamentous actin (F-actin) ring formation and pit formation. To determine F-actin ring formation, 5×10^3 cells/well were seeded in a 96-well plate, and treated with RANKL (100 ng/ml) and MFR (12.5, 25, 50 and 100 μ g/ml) at 37°C for 5 days. The medium was replaced every 2 days. The cells were fixed with 4% paraformaldehyde at room temperature for 20 min and permeabilized with 0.1% Triton X-100 in PBS at room temperature for 5 min. The cells were then stained using Acti-stain™ 488 Fluorescent Phalloidin at room temperature in the dark for 30 min. Cells were washed with PBS and nuclei were counterstained with DAPI. Images were captured using fluorescence microscopy (Cellena; Logos Biosystems; magnification, x200).

To examine pit formation, the cells were seeded in Osteo Assay Surface multiple well plates at 5×10^3 cells/well. Subsequently, the cells were treated with RANKL (100 ng/ml) and MFR (12.5, 25, 50 and 100 μ g/ml) at 37°C for 5 days. The differentiation medium was replaced every 2 days. Subsequently, cells were washed and removed using deionized water with 4% sodium hypochlorite. Images of resorbed areas were captured using an inverted light microscope (Olympus Corporation; magnification, x200). Total pit areas were analyzed using ImageJ version 1.46 (National Institutes of Health).

Western blotting. To examine the effect of MFR on osteoclast differentiation-associated transcription factors, 5×10^5 RAW 264.7 cells/well were seeded in a 60-mm dish and treated with RANKL (100 ng/ml) and MFR (12.5, 25, 50 and 100 μ g/ml) at 37°C for 1 day. In order to compare the inhibitory effect of MFR and vitexin on the expression of NFATc1 and c-Fos, 5×10^5 RAW 264.7 cells/well were seeded in a 60-mm dish and treated with RANKL (100 ng/ml) and MFR (50 and 100 μ g/ml) or vitexin (0.0753 and 0.147 μ g/ml) at 37°C for 1 day. To prepare whole-cell lysates, the cells were washed with cold DPBS, and the total proteins were extracted using RIPA lysis buffer (50 mM Tris-Cl, 150 mM NaCl, 1% NP-40, 0.5% Na-deoxycholate, 0.1% SDS, protease inhibitor cocktail, phosphatase inhibitor cocktail). Protein concentration was determined using a BCA assay. Proteins (30 μ g) were separated by SDS-PAGE on 10% gels and transferred to a nitrocellulose membrane (Whatman plc; GE Healthcare Life Sciences) according to the manufacturer's protocol. The membranes were blocked in 5% skimmed milk for 1 h at 37°C, followed by overnight incubation at 4°C with primary antibodies against NFATc1 (1:1,000), c-Fos (1:1,000), TRAF6 (1:1,000), MMP-9 (1:1,000), CTK (1:1,000) and β -actin (1:1,000). Subsequently, membranes were incubated with secondary antibodies (1:10,000) for 1 h at room temperature. The membranes were visualized using enhanced chemiluminescence reagent (cat no. RPN2106; GE Healthcare Life

Sciences) and protein expression levels were semi-quantified using ImageJ (version 1.46; National Institutes of Health).

Semi-quantitative reverse transcription-PCR (RT-PCR). To examine the effect of MFR on osteoclast-related markers, 2×10^5 cells/well seeded in a 6-well plate, and treated with the RANKL (100 ng/ml) and MFR (12.5, 25, 50 and 100 μ g/ml) at 37°C for 4 days. Total RNA of the treated cells was extracted using RNAiso Plus (cat. no. 9109; Takara Bio, Inc.) according to the manufacturer's protocol. A total of 2 μ g RNA was measured using a NanoDrop 2.0 spectrophotometer (NanoDrop; Thermo Fisher Scientific, Inc.). cDNA was synthesized using a RT kit (Invitrogen; Thermo Fisher Scientific, Inc.), according to the manufacturer's protocol. The synthesized cDNA was amplified by PCR using Taq polymerase (Kapa Biosystems; Roche Diagnostics). The PCR analysis conditions were as follows: 26–40 cycles of 30 sec at 94°C (denaturation), 30 sec at 53–58°C (annealing) and 30 sec at 72°C (extension). The primer sequences are listed in Table I. β -actin was used as a loading control. The products of qPCR were assessed on a 2% agarose gel stained with SYBR-Green (Invitrogen; Thermo Fisher Scientific, Inc.). The expression levels of mRNA were semi-quantified using ImageJ version 1.46.

Animal experimental design. To further investigate the anti-osteoporotic effects of MFR *in vivo*, an OVX rat model of menopausal osteoporosis was used. A number of 48 female Sprague Dawley (SD)-rats (age, 12 weeks; weight, 230–250 g) were obtained from KOATECH. The rats were housed in a standard environment with a controlled temperature of $22 \pm 2^\circ\text{C}$ and humidity of $55 \pm 5\%$, under a 12-h light/dark cycle. Animals were provided with *ad libitum* access to water and food. The protocol for *in vivo* experiments was approved by the Kyung Hee Medical Center Institutional Animal Care and Use Committee (KHMC-IACUC; approval no. KHMC-IACUC 19-017). All animals were allowed to acclimate for 1 week. For the postmenopausal osteoporosis model, rats were deeply anesthetized using 5% isoflurane (inhaled in 100% oxygen) and the bilateral ovaries of the rats were removed under 2–2.5% isoflurane anesthesia. The sham group underwent the same surgery to ensure they experienced the same stress, but the ovaries were not removed. No animals died during surgery. To prevent infection of the surgical site, the wound was sutured and gentamicin (4 mg/kg) was injected intraperitoneally for 3 days. After 1 week, the rats were randomly divided into six groups (n=8/group): i) Sham group, in which rats underwent the sham operation and were treated with vehicle (water); ii) OVX group, in which OVX rats were treated with vehicle; iii) E₂ group, in which OVX rats were treated with E₂ (100 μ g/kg); iv) ALN group, in which OVX rats were treated with ALN (5 mg/kg); v) MFR-L group, in which OVX rats were treated with a low dose of MFR (16.9 mg/kg); and vi) MFR-H group, in which OVX rats were treated with a high dose of MFR (169 mg/kg) for 8 weeks. E₂ and ALN were used as the positive controls. The humane endpoints used in the present study were: Dirty hair and eye discharge; self-injury and anxiety; vomiting and hemoptysis; inactivity; or anxiety and headache. None of the animals exhibited abnormal behavior.

MFR dose was calculated as follows: In Korean medicine, based on an average adult weight of 60 kg, a single dose of 8 g

Table I. Primer sequences for reverse transcription-PCR analysis.

Gene name	Sequence (5'-3')	Temperature (°C)	Cycle	Accession no.
<i>Nfatc1</i>	F: TGCTCCTCCTCCTGCTGCTC R: CGTCTTCCACCTCCACGTCG	58	32	NM_198429.2m
<i>Fos</i>	F: ATGGGCTCTCCTGTCAACAC R: GGCTGCCAAAATAAACTCCA	58	40	NM_010234.3
<i>Ctsk</i>	F: AGGCGGCTATATGACCACTG R: CCGAGCCAAGAGAGCATATC	58	26	NM_007802.4
<i>Mmp9</i>	F: CGACTTTTGTGGTCTTCCCC R: TGAAGGTTTGAATCGACCC	58	30	NM_013599.4
<i>Ca2</i>	F: CTCTCAGGACAATGCAGTGCTGA R: ATCCAGGTCACACATTCCAGCA	58	32	NM_001357334.1
<i>Acp5</i>	F: ACTTCCCCAGCCCTTACTACCG R: TCAGCACATAGCCCACACCG	58	30	NM_007388.3
<i>Atp6v0d2</i>	F: ATGGGGCCTTGCAAAGAAATCTG R: CGACAGCGTCAAACAAAGGCTTGTA	58	30	NM_175406.3
<i>Dcstamp</i>	F: TGGAAGTTCACCTGAACTACGTG R: CTCGGTTTCCCGTCAGCCTCTCTC	63	30	NM_001289506.1
<i>Oscar</i>	F: CTGCTGGTAACGGATCAGCTCCCCAGA R: CCAAGGAGCCAGAACCTTCGAAACT	53	35	NM_001290377.1
<i>Src</i>	F: TCCAGGCTGAGGAGTGGTACTTTGG R: ATACGGTAGTGAGGCGGTGACACAG	64	40	NM_001025395.2
<i>Prdm1</i>	F: TTCTTGTGTGGTATTG R: TTGGGGACACTCTTTG	50	40	NM_007548.4
<i>Actb</i>	F: TTCTACAATGAGCTGCGTGT R: CTCATAGCTCTTCTCCAGGG	58	30	NM_007393

Ctsk, cathepsin k; *Mmp9*, matrix metalloproteinase-9; *Ca2*, carbonic anhydrase 2; *Acp5*, tartrate-resistant acid phosphatase; *Atp6v0d2*, ATPase H⁺ transporting V0 subunit D2; *Dcstamp*, dendritic cell-specific transmembrane protein; *Oscar*, osteoclast-associated receptor; *Prdm1*, b lymphocyte-induced maturation protein-1; F, forward; R, reverse.

is recommended. MFR (1.016 g; yield, 12.7%) was considered equivalent to 8 g; thus, 16.9 mg MFR was required per 1 kg. Therefore, the MFR-L group was treated with 16.9 mg/kg. The MFR-H group was treated as follows: Rats are well-known to exhibit 6.4-fold faster metabolism than humans (32). *In vitro* experiments revealed that MFR exhibited a higher inhibition of osteoclast differentiation at high concentrations than at low concentrations. Based on these findings, rats in the MFR-H groups were treated with MFR at concentrations 10-fold higher than those in the MFR-L group to induce higher pharmacological effects. Therefore, the MFR-H group was treated with 169 mg/kg MFR (33-35). Oral administration was performed every morning for 8 weeks. Body weight was measured once a week and the dose was adjusted to weight. After 8 weeks, all animals were anesthetized by 5% isoflurane of inhaled anesthetics in 100% oxygen. Blood was collected using a cardiac puncture following sacrifice by cervical vertebrae dislocation. Subsequently, the uterus and femur were collected and weighed. Femurs samples were collected and fixed in 10% neutral buffered formalin for 1 day at room temperature. Uterus samples were collected and then stored at -80°C.

Serum biochemical analysis. Blood samples were incubated at room temperature for 30 min, and centrifuged at 29,739 x g

for 10 min at 4°C. Serum samples were stored at -80°C until required. Serum levels of alkaline phosphatase (ALP), aspartate aminotransferase (AST) and alanine aminotransferase (ALT) were measured by DKKorea. C-telopeptide of collagen type 1 (CTX-1) levels were measured using an ELISA kit (Elabscience; cat. no. E-EL-R1456) according to the manufacturer's protocol. TRAP levels were measured using a TRAP kit as aforementioned.

Micro-computed tomography (micro-CT) analysis. The femoral head was scanned using micro-CT (SkyScan1176; Bruker Corporation). Bone microarchitecture parameters, including bone mineral density (BMD), trabecular thickness (Tb.Th) and trabecular separation (Tb.sp) were analyzed using NRecon software (SkyScan version 1.6.10.1; Bruker Corporation).

Histological analysis. The fixed femur samples were washed using D.W at room temperature for 1 day and decalcified using 10% EDTA at room temperature for 3 weeks. Subsequently, the femur samples were dehydrated at room temperature for 1 day and embedded in paraffin. Paraffin-embedded tissues (5 μm) were sectioned on a rotary microtome (Carl Zeiss AG) and tissue sections were mounted on slides at room

temperature for 1 day. The sections on the slides were stained with hematoxylin-eosin (H&E); sections were stained with hematoxylin for 10 min and with eosin for 10 sec at room temperature. Subsequently, all slides were sealed using mounting solution and the sections were viewed under a light microscope (Olympus Corporation; magnifications, x40 and x100) for histological evaluation.

Immunohistochemistry (IHC). Paraffin-embedded tissues were deparaffinized in xylene. Endogenous peroxidases were blocked in 0.3% hydrogen peroxide at room temperature for 15 min and proteinase K (0.4 mg/ml) was used for antigen-retrieval at 37°C for 30 min. The sectioned tissues were incubated with 10% normal serum (Gibco; Thermo Fisher Scientific, Inc.) at room temperature for 1 h to block nonspecific binding, then slides were washed with PBS and incubated at 4°C for overnight with primary antibodies against NFATc1 (1:100) and CTK (1:100). The following day, the slides were washed with PBS and incubated with a secondary antibody (1:100; rabbit; cat. no: BA-1000; Vector Laboratories, Inc.) at 4°C for 1 h. The signal was visualized using an ABC kit (Vector Laboratories, Inc.) and 3, 3'-diaminobenzidine solution (Vector Laboratories, Inc.). The stained tissues were imaged using a light microscope (magnifications, x100 and x200).

MC3T3-E1 cell culture and cytotoxic assay. MC3T3-E1 cells were purchased from American Type Culture Collection. MC3T3-E1 cells were cultured in α -MEM without ascorbic acid containing 10% FBS and 1% P/S in a cell incubator at 37°C and 5% CO₂. To examine cell viability, the cells were seeded in a 24-well plate at 1x10⁴ cells/well and incubated at 37°C for 24 h. Subsequently, the cells were treated with α -MEM without ascorbic acid and MFR (12.5, 25, 50 and 100 μ g/ml) at 37°C for 24 h. Subsequently, 20 μ l/well MTS solution was added to the cells and incubated at 37°C for 2 h. Cell viability was evaluated using an ELISA reader at a wavelength of 490 nm and was expressed as a percentage of the control.

Alizarin red S staining. MC3T3-E1 cells were seeded in a 24-well plate at 1x10⁴ cells/well and incubated for 24 h. Subsequently, osteoblast differentiation was induced using osteogenic medium (α -MEM without ascorbic acid supplemented with 10 mM β -glycerophosphate, 25 μ g/ml ascorbic acid) and MFR (12.5, 25, 50 and 100 μ g/ml) at 37°C for 14 days. The medium was replaced every 2 days. The cells were then washed with DPBS, fixed with 80% ethanol at room temperature for 1 h and stained with Alizarin red S at room temperature for 5 min. To quantify mineralization, the stained dye was extracted using 10% (v/w) cetylpyridinium chloride in sodium phosphate at room temperature for 15 min. The extracted dye was measured using an ELISA reader at a wavelength of 570 nm.

Statistical analysis. Data are presented as the mean \pm standard error of the mean of three experiments. Statistical analyses were performed using GraphPad Prism version 5.01 (GraphPad Software, Inc.). *In vitro* and *in vivo* experiments were compared using a one-way ANOVA followed by a Tukey's post hoc analysis. Animal body weight was compared using a two-way

ANOVA followed by Bonferroni post hoc test. P<0.05 was considered to indicate a statistically significant difference.

Results

Quantitative analysis of the MFR extract. Vitexin was used as a standard marker of MFR, as described previously (29). The chromatogram of the MFR water extract possessed several peaks at a retention time of 0-30 min, and vitexin was observed at the same retention time as the standard (Fig. 1).

Effects of MFR on TRAP staining, and F-actin ring and pit formation. To analyze the anti-osteoporotic effect of the MFR extract *in vitro*, TRAP staining was performed using a TRAP kit. Following treatment with RANKL, TRAP staining revealed that the number of TRAP-positive cells was reduced by MFR treatment. Consistent with the results of TRAP staining, MFR decreased TRAP levels in the differentiation medium (Fig. 2A-C). As the actin ring is essential in osteoclast differentiation (36), the effect of MFR on actin ring formation was determined using immunocytochemistry. In addition, the effect of MFR on pit formation was determined using osteo-coated plates. The actin ring structures and the area of bone resorption pits were increased in the RANKL-treated cells, but were reduced following MFR treatment (Fig. 2D and E). Consistent with these results, MFR treatment reduced the number of actin rings in a dose-dependent manner (Fig. 2F). In addition, the area of bone resorption pits was significantly reduced following MFR treatment (Fig. 2G). To confirm whether the concentration of MFR used in the *in vitro* experiments affected the viability of RAW 264.7 cells, the cells were treated with 12.5-100 μ g/ml MFR. MFR did not affect the viability of RAW 264.7 cells or mature osteoclasts (Fig. 2H and I). In addition, the present study compared and analyzed the inhibitory effect of MFR and vitexin on osteoclast differentiation to determine if the ability of MFR to inhibit osteoclast differentiation was associated with vitexin. The content of vitexin in MFR was 1.47 ppm (0.147%); 0.147 μ g/ml vitexin in 100 μ g/ml MFR and 0.0753 μ g/ml vitexin in 50 μ g/ml MFR. The effects of the two substances (MFR and vitexin) on TRAP staining and TRAP levels in the medium were subsequently assessed. To confirm whether the concentration of vitexin contained in MFR affects the osteoclast inhibitory effect, TRAP staining was performed. As shown in Fig. S1A and B, TRAP-positive cells and TRAP levels were increased in the RANKL-treated cells. Conversely, the number of TRAP-positive cells was considerably decreased by MFR (50 and 100 μ g/ml) treatment compared with vitexin (0.0753 and 0.147 μ g/ml). Similarly, MFR (50 and 100 μ g/ml) further decreased TRAP levels compared with vitexin (0.0753 and 0.147 μ g/ml) (Fig. S1B).

To determine whether the concentration of vitexin contained in MFR affects the inhibitory effect on transcription factors, NFATc1 and c-Fos were measured using western blotting. The protein expression levels of NFATc1 and c-Fos were increased by RANKL treatment. MFR (50 and 100 μ g/ml) inhibited the expression of NFATc1 and c-Fos compared with vitexin (0.0753 and 0.147 μ g/ml) (Fig. S1C and D). To confirm whether the concentration of vitexin used in experiments affected the viability of RAW 264.7 cells, the cells were treated with vitexin (0.0753 and 0.147 μ g/ml); vitexin

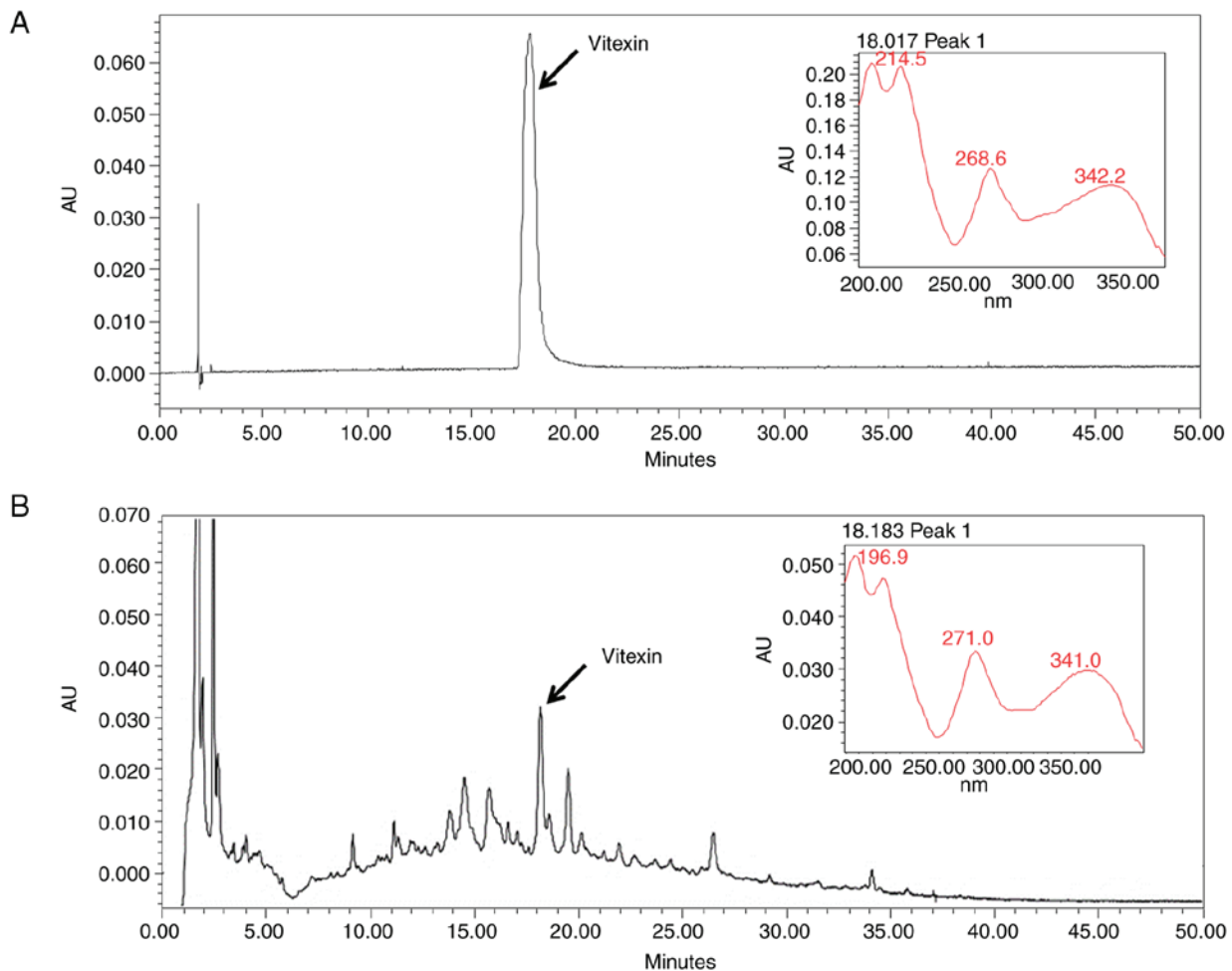


Figure 1. High-performance liquid chromatography analysis of the MFR extracts. Vitexin was confirmed in (A) the standard and (B) MFR water extract at a wavelength of 335 nm. MFR, *Melandrium firmum* Rohrbach.

not affect cell cytotoxicity (Fig. S1E). Taken together, it was revealed that the osteoclast inhibitory effect of MFR was not mediated by vitexin.

Effect of MFR on protein and mRNA expression levels of NFATc1 and c-Fos. NFATc1 and c-Fos are important transcription factors required for mature osteoclast differentiation in RAW 264.7 cells (37,38). RANKL-induced expression of NFATc1 and c-Fos was measured using western blotting and RT-qPCR. Treatment with RANKL significantly increased the expression levels of NFATc1, whereas MFR decreased the protein and mRNA expression levels of NFATc1 (Fig. 3A and B). In addition, c-Fos expression was significantly increased by RANKL treatment, whereas this increase was reversed by MFR treatment (Fig. 3C and D). Furthermore, RANKL stimulation increased TRAF6, but this finding was not significant, and treatment of MFR attenuated the increased expression of TRAF6. In particular, in cells treated with 25 μ g/ml MFR, the expression of TRAF6 was significantly decreased compared with that in RANKL-only treated cells (Fig. 3E and F).

Effect of MFR on RANKL-induced expression of bone resorption and osteoclast-related markers. The inhibitory effects of the MFR extract on bone resorption markers were examined

using western blotting and RT-qPCR. Treatment with RANKL significantly increased the expression levels of MMP-9 and CTK, whereas MFR decreased the protein expression levels of MMP-9 and CTK (Fig. 4A and B). Consistent with the results of western blotting, MFR reduced the mRNA expression levels of *Mmp9*, *Ctsk* and carbonic anhydrase 2 (*CA2/Ca2*) (Fig. 4C and D). In addition, the effects of MFR on RANKL-stimulated changes in osteoclast-specific genes, including *Acp5*, *Atp6v0d2*, dendritic cell-specific transmembrane protein (*DC-STAMP/Dcstamp*), *Oscar*, c-Src (*Src*) and B lymphocyte-induced maturation protein-1 (*Blimp-1/Prdm1*), were determined, as they are crucial in promoting osteoclastogenesis (39). The mRNA expression levels of osteoclast-specific genes were increased by RANKL treatment, whereas MFR attenuated the RANKL-induced increase in the mRNA expression levels of osteoclast-specific genes, including *Acp5*, *Atp6v0d2*, *Dcstamp*, *Oscar*, *Src* and *Prdm1*, in a dose-dependent manner (Fig. 4E-H).

Effect of MFR on body, uterus and femur weights, and on the levels of hepatotoxicity, bone formation and bone resorption markers. As shown in Fig. 5A, the OVX group exhibited a significant increase in body weight compared with that in the sham group from 4 weeks. The E₂ group had a significantly lower increase in body weight after 3 weeks compared with

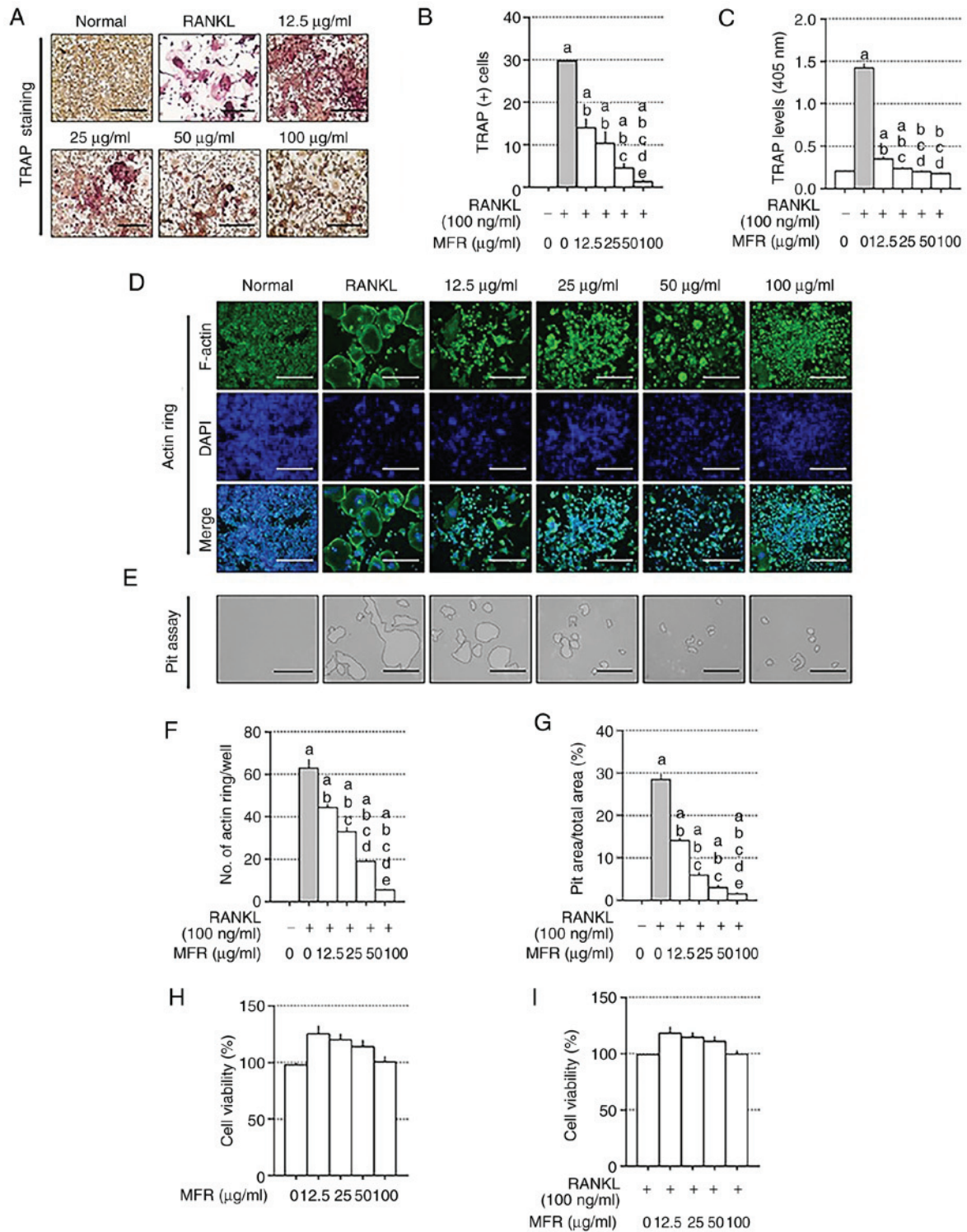


Figure 2. Effect of MFR on RANKL-induced osteoclast differentiation, F-actin ring formation and pit formation. (A) RANKL-induced osteoclasts were stained using a TRAP kit. Magnification, x100; scale bar, 200 μm . (B) Number of TRAP-positive cells with >3 nuclei were counted. (C) TRAP levels was measured using an enzyme-linked immunosorbent assay reader. (D) F-actin rings were stained using fluorescent phalloidin and (E) a bone resorption assay was performed using osteo-coated plates. Magnification, x100; scale bar, 200 μm . (F) Number of F-actin rings was counted and (G) pit area was measured using ImageJ. (H) RAW 264.7 cell viability was determined using the MTS assay. (I) Cell viability of mature osteoclasts was examined using the MTS assay. All data are presented as the mean \pm standard error of the mean of three independent experiments. Data were analyzed using one-way ANOVA followed by Tukey's post hoc test. ^aP<0.05 vs. normal group (untreated cells); ^bP<0.05 vs. RANKL treatment group; ^cP<0.05 vs. MFR 12.5 $\mu\text{g/ml}$ treatment group; ^dP<0.05 vs. MFR 25 $\mu\text{g/ml}$ treatment group; ^eP<0.05 vs. MFR 50 $\mu\text{g/ml}$ treatment group. MFR, *Melandrium firmum* Rohrbach; RANKL, receptor activator of nuclear factor- κB ligand; F-actin, filamentous actin; TRAP, tartrate-resistant acid phosphatase.

the OVX group; however, MFR-L, MFR-H and ALN treatment did not affect body weight. In addition, the OVX group exhibited significantly decreased uterus weight compared

with that in the sham group, whereas E₂ treatment prevented uterus weight loss. MFR-L, MFR-H and ALN groups did not exhibit any protective effects on uterus weight loss (Fig. 5B).

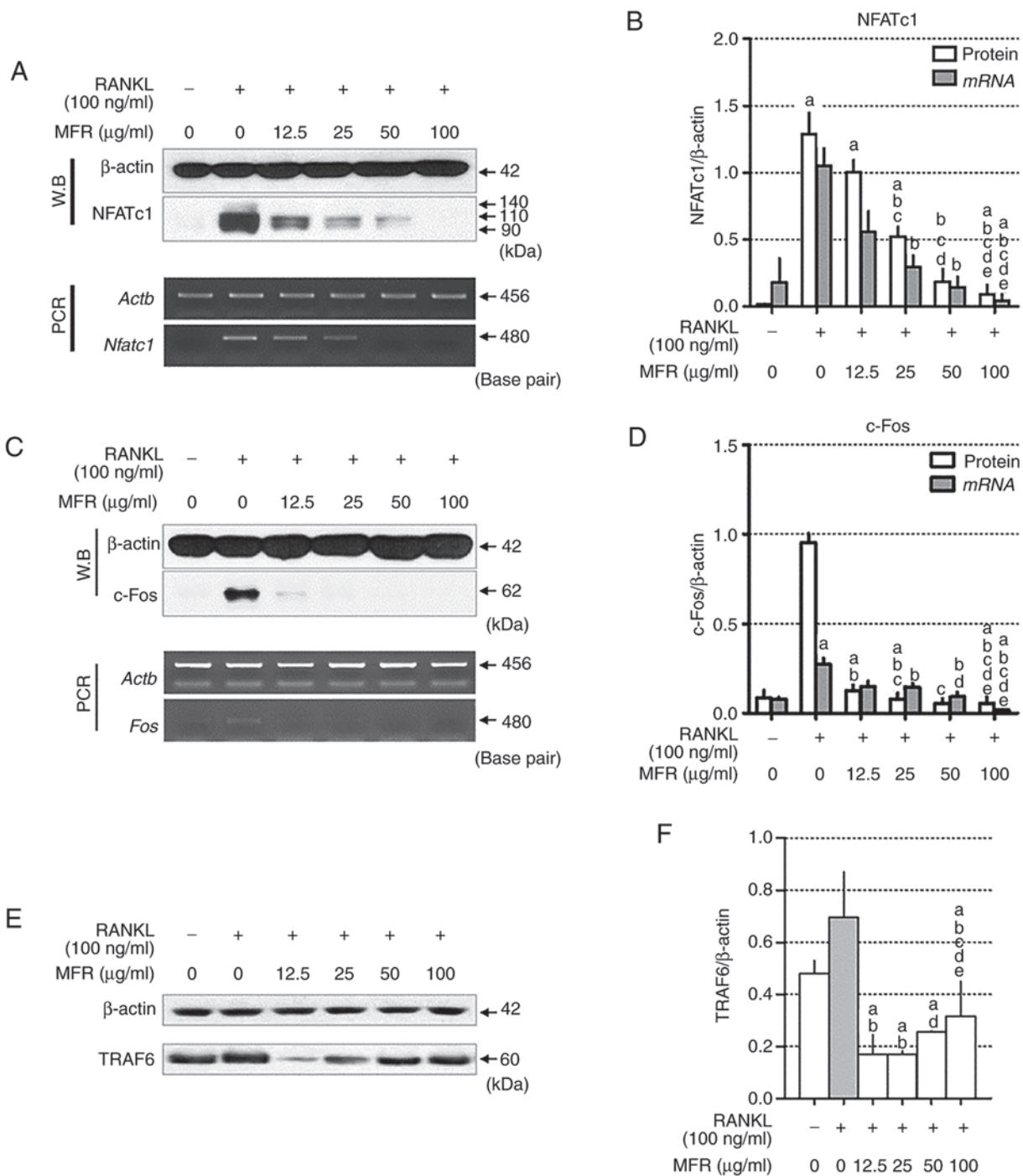


Figure 3. Effect of MFR on the protein and mRNA expression levels of NFATc1, c-Fos and TRAF6. (A) NFATc1 expression was determined by western blotting and reverse transcription-PCR, and (B) normalized to β -actin. (C) Protein and mRNA expression levels of c-Fos were determined and (D) normalized to β -actin. (E) Protein expression levels of TRAF6 were measured and (F) normalized to β -actin. Data are presented as the mean \pm standard error of the mean of three independent experiments. All data were analyzed using one-way ANOVA followed by Tukey's post hoc test. ^a $P < 0.05$ vs. normal group (untreated cells); ^b $P < 0.05$ vs. RANKL treatment group; ^c $P < 0.05$ vs. MFR 12.5 $\mu\text{g/ml}$ treatment group; ^d $P < 0.05$ vs. MFR 25 $\mu\text{g/ml}$ treatment group; ^e $P < 0.05$ vs. MFR 50 $\mu\text{g/ml}$ treatment group. MFR, *Melandrium firmum* Rohrbach; RANKL, receptor activator of nuclear factor- κ B ligand; NFATc1, nuclear factor of activated T-cells; TRAF6, tumor necrosis factor receptor-associated factor 6.

While E_2 and ALN groups exhibited a preventive effect on the reduction of femur weight compared with the OVX group, MFR-L and MFR-H groups did not (Fig. 5C). To investigate the extent of hepatotoxicity following treatment with MFR, E_2 and ALN, the serum levels of AST and ALT were measured. Previous studies have shown that levels above 150 U/l for AST and 40 U/l for ALT indicate hepatotoxicity in rats (40,41). The

levels of AST and ALT in the MFR-L, MFR-H, E_2 and ALN groups in the present study did not exceed these values; therefore, it was indicated that MFR-L, MFR-H, E_2 and ALN did not induce hepatotoxicity (Fig. 5D and E). To determine the effect of MFR on bone formation, the serum levels of ALP were measured. ALP was significantly increased in the OVX group compared with that in the sham group; moreover, the MFR-L

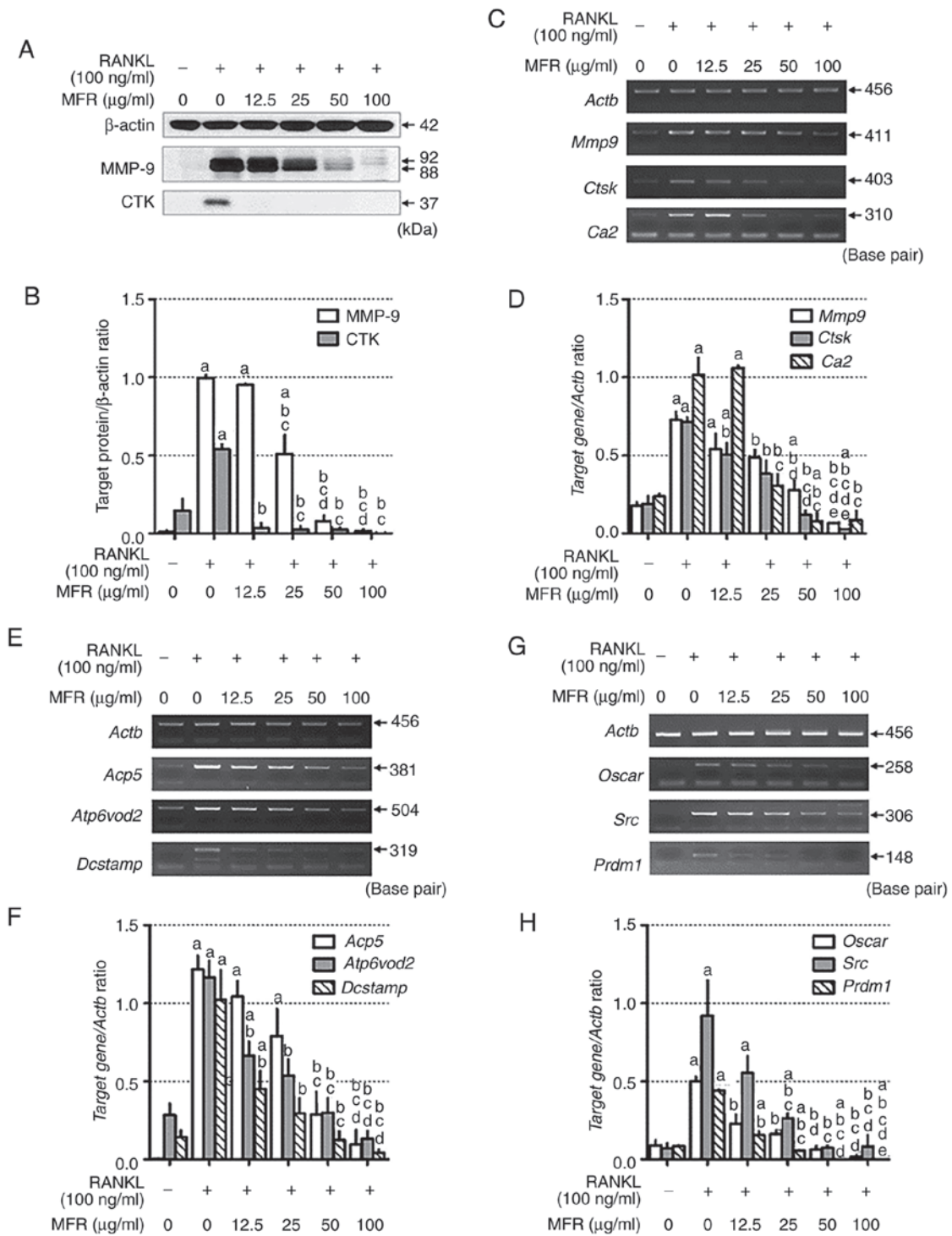


Figure 4. Effect of MFR on the expression levels of osteoclast-related genes. (A) Western blot analysis of CTK and MMP-9. (B) Protein expression levels were normalized to β -actin. (C) mRNA expression levels of *Mmp9*, *Ctsk* and *Ca2* were analyzed using RT-PCR. (D) mRNA expression levels were normalized to *Actb*. (E) RT-PCR analysis was used to determine the mRNA expression levels of *Acp5*, *Atp6v0d2* and *Dcstamp*, and (F) expression was normalized to *Actb*. (G) RT-PCR analysis was performed to determine the mRNA expression levels of *Oscar*, *Src* and *Prdm1*, and (H) expression was normalized to *Actb*. All data are presented as the mean \pm standard error of the mean of three independent experiments. Data were analyzed using one-way ANOVA followed by Tukey's post hoc test. ^aP<0.05 vs. normal group (untreated cells); ^bP<0.05 vs. RANKL treatment group; ^cP<0.05 vs. MFR 12.5 μ g/ml treatment group; ^dP<0.05 vs. MFR 25 μ g/ml treatment group; ^eP<0.05 vs. MFR 50 μ g/ml treatment group. MFR, *Melandrium firmum* Rohrbach; RANKL, receptor activator of nuclear factor- κ B ligand; CTK/*Ctsk*, cathepsin k; MMP-9/*Mmp9*, matrix metalloproteinase-9; CA2/*Ca2*, carbonic anhydrase 2; RT-PCR, reverse transcription-PCR; *Acp5*, tartrate-resistant acid phosphatase; *Atp6v0d2*, ATPase H⁺ transporting V0 subunit D2; *Dcstamp*, dendritic cell-specific transmembrane protein; *Oscar*, osteoclast-associated receptor; *Prdm1*, B lymphocyte-induced maturation protein-1.

group exhibited decreased serum levels of ALP, whereas the MFR-H, E₂ and ALN groups did not (Fig. 5F). To examine the effect of MFR on bone resorption, serum levels of CTX-1

and TRAP were measured. CTX-1 levels were increased in the OVX group compared with those in the sham group, whereas they were significantly decreased in the MFR-L, E₂ and ALN

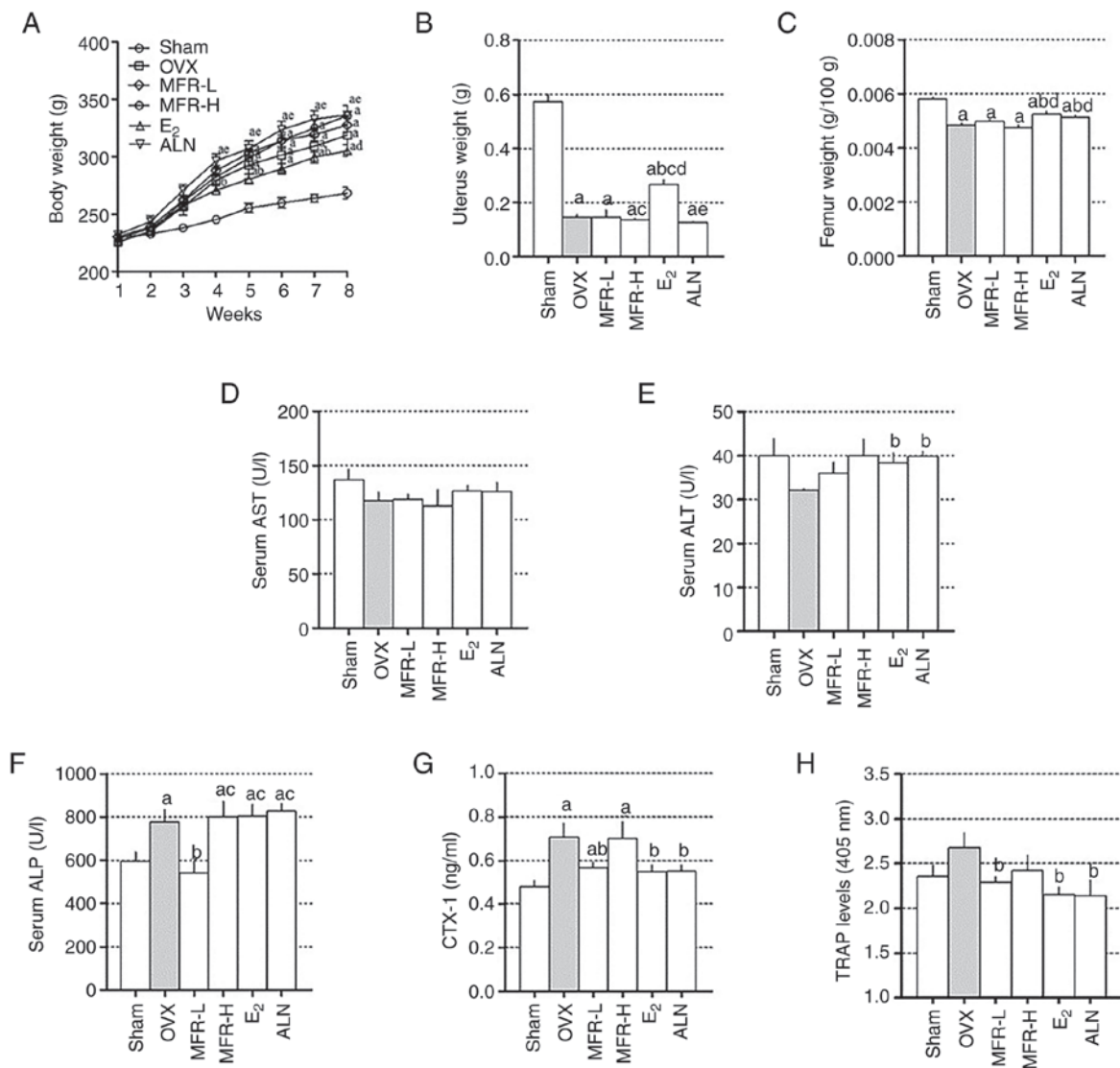


Figure 5. Effect of MFR on body, uterus and femur weights, and serum levels of ALP, AST and ALT. (A) Body weight was measured weekly for 8 weeks. (B) Uterus and (C) femur weights were measured after sacrificing the rats. The serum levels of (D) AST, (E) ALT, (F) ALP, (G) CTX-1 and (H) TRAP were measured using enzyme-linked immunosorbent assays. All data are presented as the mean \pm standard error of the mean ($n=8$ per group). (A) Data were analyzed using two-way ANOVA followed by Bonferroni post hoc test. (B-H) Data were analyzed using one-way ANOVA followed by Tukey post hoc test. ^a $P<0.05$ vs. sham group; ^b $P<0.05$ vs. OVX group; ^c $P<0.05$ vs. MFR-L group; ^d $P<0.05$ vs. MFR-H group; ^e $P<0.05$ vs. E_2 group. MFR, *Melandrium firmum* Rohrbach; OVX, ovariectomized; ALP, alkaline phosphatase; AST, aspartate aminotransferase; ALT, alanine aminotransferase; CTX-1, C-telopeptide of type I collagen; TRAP, tartrate-resistant acid phosphatase; MFR-L, low dose of MFR; MFR-H, high dose of MFR; E_2 , β -estradiol; ALN, alendronate.

groups compared with those in the OVX group; there were no significant changes in the MFR-H group (Fig. 5G). As shown in Fig. 5H, TRAP levels were increased due to OVX, but the difference was not significant, whereas oral administration of MFR-L, E_2 and ALN reduced TRAP levels. Furthermore, the TRAP levels were decreased in the MFR-H group; however, this finding was not significant.

Effect of MFR on the bone microarchitecture of ovariectomy-induced osteoporosis in rats. In order to investigate the protective effects of MFR on ovariectomy-induced bone loss, micro-CT was used. As shown in Fig. 6A, micro-CT images of the femoral head indicated trabecular bone loss in OVX rats. BMD loss was significantly inhibited in the MFR-L, E_2 and ALN groups compared with that in the OVX group (Fig. 6B). Furthermore, Tb.Th in the OVX group was

reduced compared with that in the sham group, whereas Tb.Th was significantly increased in the ALN group. However, Tb.Th in the MFR-L, MFR-H and E_2 groups did not differ significantly from that in the OVX group (Fig. 6C). As shown in Fig. 6D, Tb.sp was significantly increased in the OVX group compared with that in the sham group, whereas Tb.sp levels were decreased in the E_2 and ALN groups. However, Tb.sp levels were not affected in the MFR-L and MFR-H groups.

Effect of MFR on bone loss in the OVX rat model of osteoporosis. To investigate the histological changes in the femoral head, H&E staining was performed on the bone tissue (Fig. 7A). The trabecular area in the femoral head of OVX rats was significantly decreased compared with that in the sham group, whereas this reduction was prevented by treatment with MFR-L, E_2 and ALN (Fig. 7B).

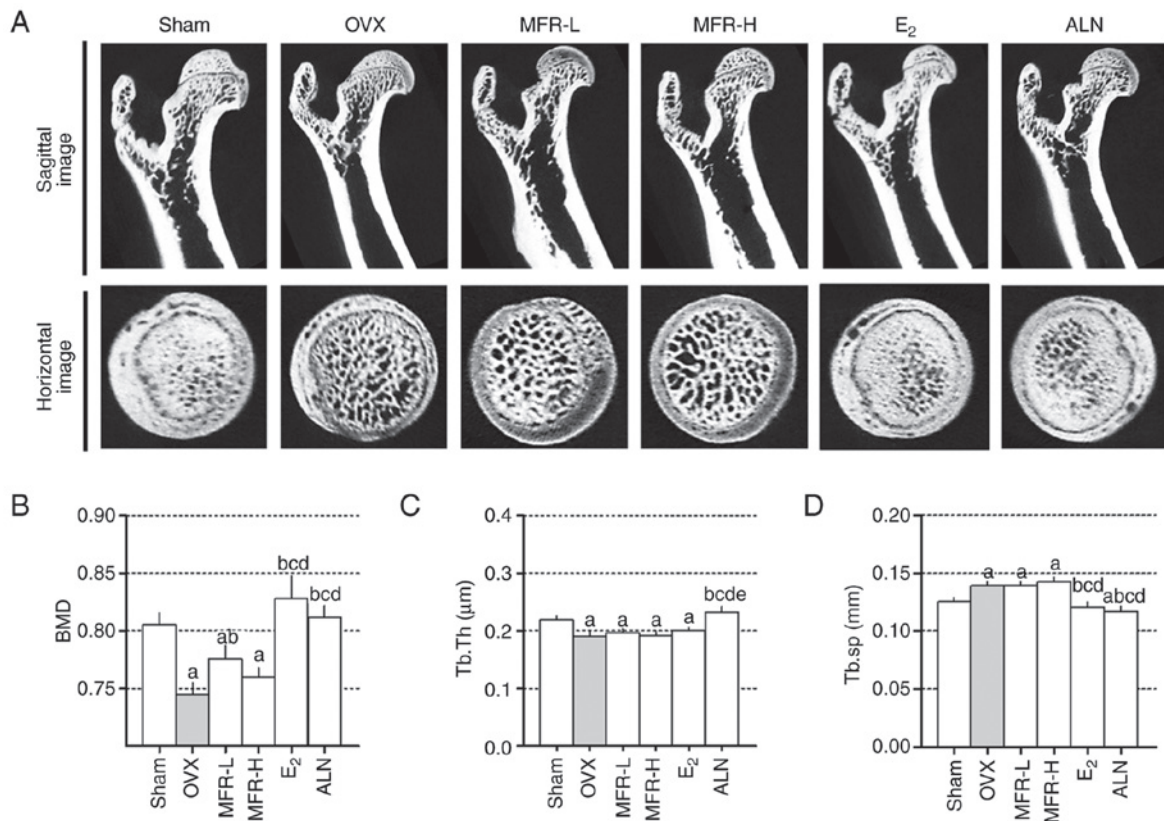


Figure 6. Effects of MFR on bone microarchitecture of OVX-induced osteoporosis rats. (A) Femurs were analyzed using micro-CT imaging. (B) BMD, (C) Tb.Th and (D) Tb.sp were analyzed using micro-CT image analysis. All data are presented as the mean \pm standard error of the mean (n=8/group). Statistical analyses were performed using one-way ANOVA followed by Tukey post hoc test. ^aP<0.05 vs. sham group; ^bP<0.05 vs. OVX group; ^cP<0.05 vs. MFR-L group; ^dP<0.05 vs. MFR-H group; ^eP<0.05 vs. E₂ group. MFR, *Melandrium firmum* Rohrbach; OVX, ovariectomized; BMD, bone mineral density; Tb.Th, trabecular thickness; Tb.sp, trabecular spacing; micro-CT, micro computed tomography; MFR-L, low dose of MFR; MFR-H, high dose of MFR; E₂, β -estradiol; ALN, alendronate.

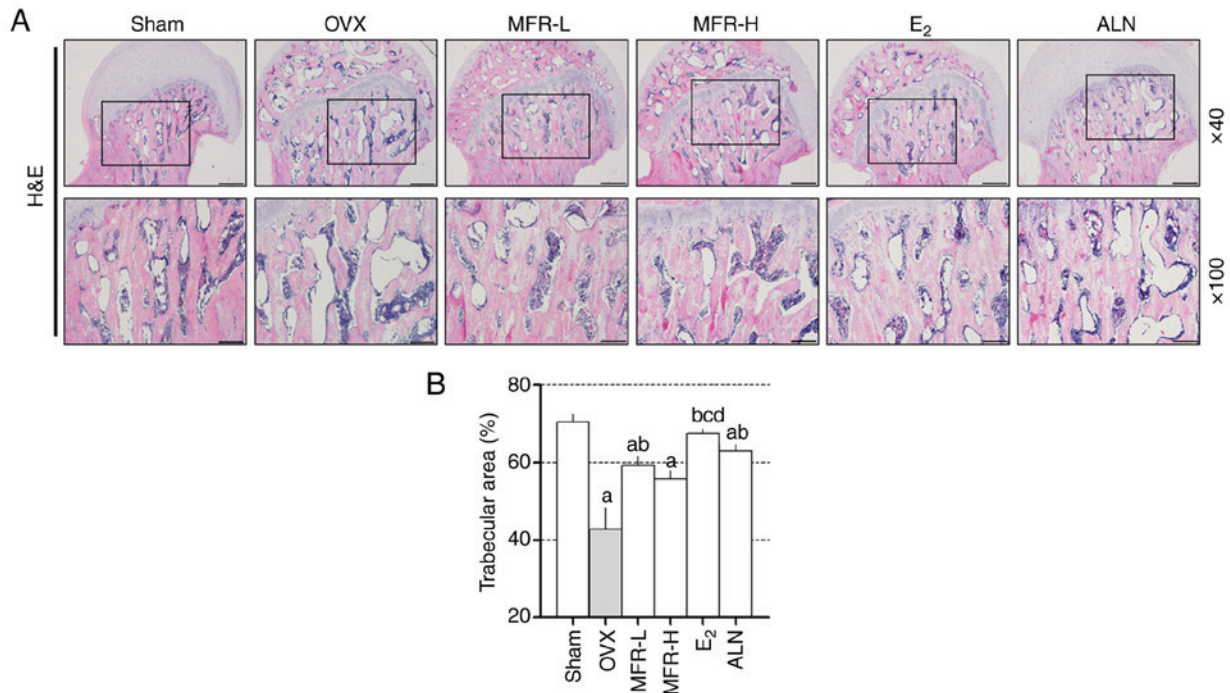


Figure 7. Effect of MFR on trabecular area in OVX-induced rats. (A) Bone tissues were stained with H&E. Magnifications, x40 and x100; scale bar, 500 and 200 μ m, respectively. (B) Trabecular area was analyzed in the H&E-stained sections. All data are presented as the mean \pm standard error of the mean (n=8/group). Statistical analyses are performed using one-way ANOVA followed by Tukey post hoc test. ^aP<0.05 vs. sham group; ^bP<0.05 vs. OVX group; ^cP<0.05 vs. MFR-L group; ^dP<0.05 vs. MFR-H group. MFR, *Melandrium firmum* Rohrbach; OVX, ovariectomized; H&E, hematoxylin and eosin; MFR-L, low dose of MFR; MFR-H, high dose of MFR; E₂, β -estradiol; ALN, alendronate.

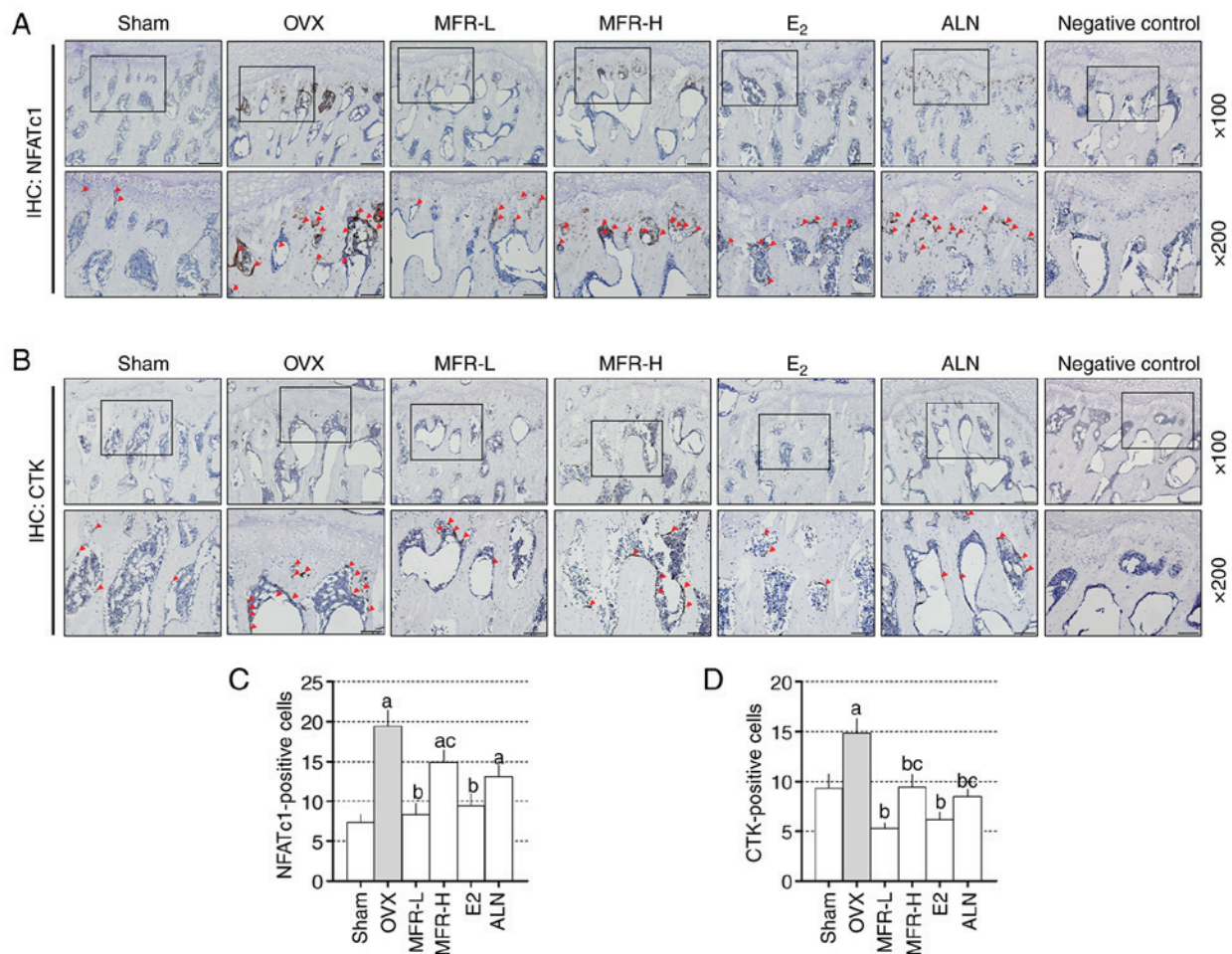


Figure 8. Effects of MFR on the expression levels of CTK and NFATc1 in OVX-induced rats. (A) NFATc1 and (B) CTK-positive expression in bone tissue was assessed using IHC. NFATc1 and CTK-positive expression is highlighted by the red arrowheads. Mean number of (C) NFATc1 and (D) CTK-positive cells in femur tissues was counted. Magnifications, x100 and x200; scale bar, 200 and 100 μ m, respectively. All data are presented as the mean \pm standard error of the mean (n=8/group). Statistical analyses are performed using one-way ANOVA followed by Tukey post hoc test. ^aP<0.05 vs. sham group; ^bP<0.05 vs. OVX group; ^cP<0.05 vs. MFR-L group. MFR, *Melandrium firmum* Rohrbach; CTK, cathepsin k; NFATc1, nuclear factor of activated T-cells, cytoplasmic 1; OVX, ovariectomized; IHC, immunohistochemistry; MFR-L, low dose of MFR; MFR-H, high dose of MFR; E₂, β -estradiol; ALN, alendronate.

Effect of MFR on the expression levels of NFATc1 and CTK in femoral tissues in the in vivo osteoporosis model. To determine the effect of MFR on the expression levels of NFATc1 and CTK in the rat model of osteoporosis, IHC was performed (Fig. 8A and B). The OVX group exhibited increased expression levels of NFATc1 compared with those in the sham group. By contrast, the MFR-L and E₂ groups exhibited significantly reduced expression levels of NFATc1 expression; no changes were observed in the MFR-H and ALN groups compared with the OVX group (Fig. 8C). In OVX rats, the expression levels of CTK were increased compared with those in the sham group. Conversely, MFR-L, MFR-H, E₂ and ALN effectively reduced the expression levels of CTK (Fig. 8D).

Effect of MFR on mineralization of MC3T3-E1 cells. MC3T3-E1 cells derived from mouse calvaria are characterized by proliferation, differentiation and mineralization of osteoblasts, and are used in studies related to bone formation (42). Alizarin red staining can be used to detect the formation of mineralization (43). Therefore, to confirm the effect of MFR on osteoblast differentiation and mineralization, Alizarin red S staining was performed. The control cells exhibited

significantly increased mineralization compared with that in the normal cells. Treatment with low concentrations of MFR (12.5 and 25 μ g/ml) promoted osteoblast differentiation, but high concentrations of MFR (50 and 100 μ g/ml) inhibited osteoblast differentiation (Fig. 9A). To examine the effects of the MFR extract on MC3T3-E1 cell viability, cells were treated with 12.5-100 μ g/ml MFR. Notably, MFR did not affect the viability of MC3T3-E1 cells (Fig. 9B). Quantification of Alizarin red staining revealed a significantly reduced effect of MFR in a dose-dependent manner (Fig. 9C).

Discussion

The aim of the present study was to investigate the inhibitory effect of MFR extract on osteoclast differentiation and bone loss in ovariectomy-induced postmenopausal osteoporotic rats. *In vitro*, MFR inhibited RANKL-induced osteoclast differentiation, formation and function. In addition, MFR inhibited the TRAF6 axis and inhibited the expression of NFATc1/c-Fos, which is known as a key factor for osteoclast differentiation. Finally, MFR suppressed the expression of osteoclast-related genes, such as *Acp5*, *Mmp9*, *CtsK*, *Atp6v0d2*, *Dcstamp* and *Src*;

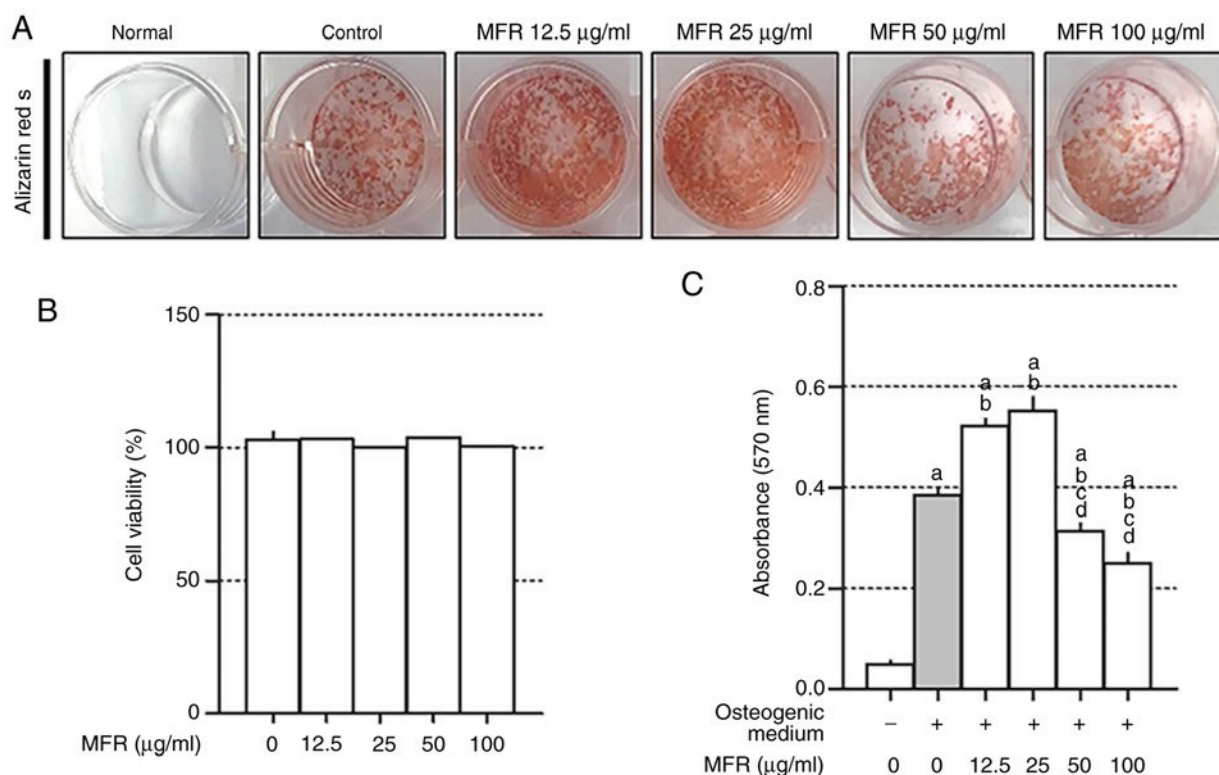


Figure 9. Effects of MFR on the production of mineralization in MC3T3-E1 cells. (A) MFR treatment suppressed mineralization in MC3T3-E1 cells. (B) Cell viability was determined using the MTS assay. (C) Quantitative analysis of mineralization was performed using an enzyme-linked immunosorbent assay reader. Data were analyzed using one-way ANOVA followed by Tukey's post hoc test. ^aP<0.05 vs. normal group (untreated cells); ^bP<0.05 vs. osteogenic medium treatment group; ^cP<0.05 vs. MFR 12.5 µg/ml treatment group; ^dP<0.05 vs. MFR 25 µg/ml treatment group; MFR, *Melandrium firmum* Rohrbach.

this potential mechanism of suppression is shown in Fig. 10. *In vivo*, MFR-L considerably increased BMD, trabecular area, and decreased the expression levels of NFATc1 and CTK in OVX-induced models.

Murine macrophage RAW 264.7 cells have a monocyte/macrophage like cell lineage; they are derived from BALB/c mice (44) and are suitable as a cell experimental model in measuring osteoclast differentiation (45). TRAP staining is the standard method used to detect osteoclast formation and levels (31,46,47). In the present study, MFR suppressed RANKL-induced TRAP-positive cells and TRAP levels. The F-actin ring is the cytoskeletal structure that is required for formation of the sealing zone, and permits the firm adhesion of mature osteoclasts to the bone surface (48). The pit formation assay is widely used to examine bone resorption and is an important indicator of bone resorption from mature osteoclasts (48-50). In the present study, MFR reduced the number and size of the F-actin rings and the area of pit formation in RANKL-induced cells. These results suggested that MFR may inhibit osteoclast formation and bone resorption.

The RANK/RANKL signaling pathway has been reported to induce the activation of TRAF6. TRAF6 deficiency in mice is known to induce severe osteopetrosis and impairment in osteoclast function (51-53). Activated TRAF6 can stimulate c-Fos, which serves a crucial role in the induction of transcription factors, including NFATc1 (54-56). In a previous study, c-Fos-knockout mice developed osteopetrosis due to attenuated osteoclast function (20). In addition, NFATc1-deficient adult mice exhibited reduced bone loss in the absence of

osteoclast activity (17,19). In the present study, MFR was shown to reduce the protein and mRNA expression levels of c-Fos and NFATc1. These results suggested that MFR may decrease the production of osteoclast differentiation, bone resorption and F-actin ring formation by suppressing NFATc1 and c-Fos signaling pathways. However, in contrast to the results regarding NFATc1/c-Fos, the present study revealed that MFR significantly inhibited TRAF6 at low concentrations but not at high concentrations. The reason for the difference in the expression levels of each factor can be inferred due to the following reasons. RANKL binds to RANK, increases the expression and ubiquitination of TRAF6, and leads to the accumulation of the TRAF6/transforming growth factor-β-activated kinase 1 (TAK1) complex, which activates sub-signaling molecules, such as phosphoinositide 3-kinases, MAPK and NF-κB (57,58). It was hypothesized that treatment with a high concentration of MFR in the present study could inhibit the ubiquitination of TRAF6 or the accumulation of the TRAF6/TAK1 complex, rather than affecting the expression of TRAF6. However, additional research needs to be conducted to assess this hypothesis.

NFATc1 regulates several important osteoclast-related genes, such as *Mmp9*, *Ctsk* and *Ca2*, which are markers of bone resorption (17). *Mmp9* and *Ctsk* are well-known as bone resorption enzymes. Notably, *Mmp9* is expressed during the transformation of early osteoclasts to mature osteoclasts (59) and deficiency of *Ctsk* leads to impairments in bone resorption in mice and humans (60). Furthermore, *Ca2* is an enzyme that is upregulated by c-Fos signaling, and is expressed in the early

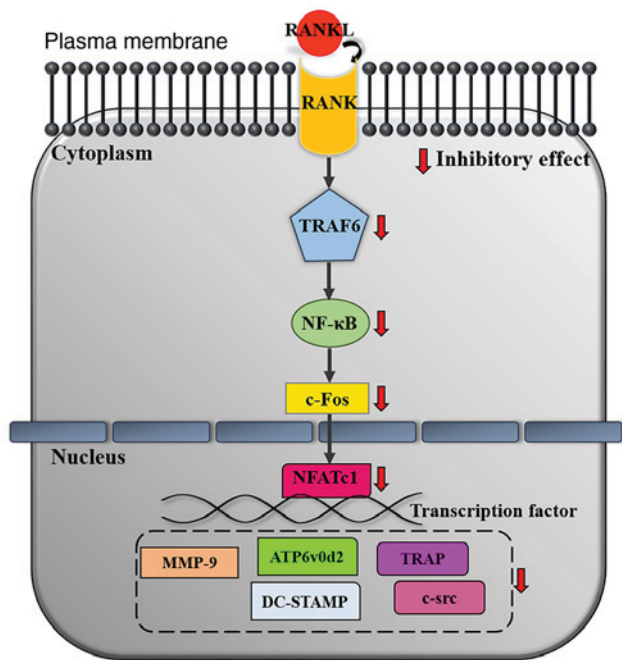


Figure 10. Inhibitory mechanisms of MFR on osteoclast differentiation. MFR, *Melandrium firmum* Rohrbach; RANKL, receptor activator of nuclear factor- κ B ligand; RANK, receptor activator of nuclear factor- κ B; TRAF6, tumor necrosis factor receptor-associated factor 6; NF- κ B, nuclear factor- κ B; NFATc1, nuclear factor of activated T cells, cytoplasmic 1; MMP-9, matrix metalloproteinase-9; ATP6v0d2, ATPase H⁺ transporting V0 subunit D2; DC-STAMP, dendritic cell-specific transmembrane protein; TRAP, tartrate-resistant acid phosphatase.

stages of osteoclast differentiation and influences the acidity of the bone surface (61). In the present study, MFR suppressed the expression levels of *mmp9*, *ctsk* and *ca2*. These results suggested that MFR may possess anti-osteoporotic activity by regulating the expression of bone resorption markers. *Atp6vod2* and *Dcstamp* serve an important role in cell-cell fusion during RANKL-stimulated osteoclast differentiation. In addition, *Atp6vod2* and *Dcstamp* are important for F-actin ring formation (39,62). Notably, gene-knockout mice of *Atp6vod2* and *Dcstamp* have been reported to develop osteopetrosis due to defects in osteoclastogenesis (62,63). In the present study, MFR suppressed the expression levels of *Atp6vod2* and *Dcstamp*. These results indicated that the inhibitory effect of MFR on F-actin ring formation may be associated with the suppression of *Atp6vod2* and *Dcstamp*. *Oscar* serves an important role in the bone-specific regulation of osteoclast differentiation, and activation of *Oscar* results in differentiation of early osteoclasts to mature osteoclasts. In addition, *Oscar* can induce calcium activation, resulting in increased expression of NFATc1 (64). *Src* signaling is important in regulating the osteoclast cytoskeleton (65). *Prdm1* serves an essential role in the differentiation and functions of macrophages and lymphocytes (66). In addition, *Prdm1* controls osteoclast development and bone homeostasis (67). In the present study, MFR decreased the expression levels of *Oscar*, *Src* and *Prdm1*. These results suggested that MFR may inhibit the expression of osteoclast-related genes by suppressing NFATc1 signaling. Notably, several genes were expressed in the form of two bands in the present study; as a result of comparing the primer size using a DNA ladder marker, the band at the top is considered

the target, and the bottom is inferred as the dimer remaining after the reaction was completed.

Osteoporosis is the most common type of bone disease worldwide, which is characterized by a low bone mass (68). Estrogen deficiency is the primary cause of postmenopausal osteoporosis (69). Rats with ovariectomy-induced osteoporosis have been used as a postmenopausal osteoporosis model and share clinical characteristics with human osteoporosis (3). It has been established that an increase in body weight is a symptom observed in OVX rats. In addition, reduction in uterus weight is indicative of successful establishment (70). In the present study, the body weight of animals was significantly increased 3 weeks after OVX and uterus weight was significantly decreased in the OVX group compared with that in the sham group. These results suggested that a postmenopausal osteoporosis model was successfully established.

ALP is a marker commonly associated with bone formation, which is produced during the early differentiation of osteoblasts (71). Wu *et al* (72) demonstrated that ALP activity was increased in estrogen-deficient mice. Excessive osteoclast activity causes an imbalance in bone metabolism, resulting in increased osteoblast activity and ALP expression. In the present study, the serum ALP levels were significantly increased in the OVX group compared with those in the sham group, whereas ALP levels were significantly decreased in the MFR-L group. These results suggested that the MFR-L group reduced the levels of ALP, which were increased due to excessive osteoclast activity. AST and ALT are the most commonly used factors for assessment of hepatotoxicity (73). The results of the present study suggested that the levels of AST and ALT were not affected in OVX rats. In addition, MFR-L, MFR-H, E₂ and ALN did not exert hepatotoxic effects. CTX is the most widely used indicator to measure bone resorption, and CTX-1 and TRAP are bone resorption markers of osteoclasts that have been reported to be increased in OVX models (74). In the present study, CTX-1 levels were significantly increased in the OVX group, whereas they were reduced in the MFR-L, E₂ and ALN groups; CTX-1 levels in the MFR-H group were unchanged. In addition, TRAP levels were increased in the OVX group; however, this difference was not significant. By contrast, TRAP levels were reduced in the MFR-L, E₂ and ALN groups; TRAP levels were also reduced in the MFR-H group, but this change was not significant.

Micro-CT has been used to study bone tissues and in orthopedic studies (75). The advantage of micro-CT is the lack of damage to the sample and ease of reconstruction using image sections (76). BMD refers to the amount of mineral content in bone tissue and is indicative of the strength of bones; BMD is based on calcium content and is an important measure in the evaluation of the OVX rat model (77). In the present study, the BMD in the OVX group was significantly decreased compared with that in the sham group, whereas BMD loss was reduced in the MFR-L, E₂ and ALN groups. Tb.Th and Tb.sp are indicators used in assessment of the 3D image structure of cancellous bone (78). In the present study, the results revealed that the OVX group exhibited decreased Tb.Th and increased Tb.sp compared with those in the sham group. Tb.Th was increased following ALN treatment compared with that in the OVX group, but no significant effect was observed on Tb.Th in the OVX rats treated with MFR-L, MFR-H and E₂. Tb.sp

was decreased in the E₂ and ALN groups compared with that in the OVX group, but no significant effect was observed in the MFR-L and MFR-H groups. These findings indicated that oral administration of MFR-L reduced bone loss.

Decreased trabecular area is a symptom commonly observed in patients with osteoporosis and is the primary cause of an increased risk of fracture; thus, the trabecular area has been used as an important index of anti-osteoporotic activity in a previous study (79). H&E staining can also be used to assess the trabecular area in the femur alongside micro-CT (80-84). Bone loss of the femoral head was enhanced in the OVX rats, whereas MFR-L, E₂ and ALN reduced trabecular area loss in the OVX-induced rat models. These results suggest that MFR-L, E₂ and ALN inhibited OVX-induced bone loss. IHC demonstrated that the expression levels of NFATc1 were decreased following treatment with MFR-L and E₂. In addition, administration of MFR-L, MFR-H, E₂ and ALN reduced the expression levels of CTK in the OVX rats.

The present study confirmed the effect of MFR on osteoblast differentiation, which has an important role in bone metabolism. MFR (12.5 and 25 µg/ml) promoted osteoblast differentiation, whereas MFR (50 and 100 µg/ml) suppressed osteoblast differentiation. These results indicated that high concentrations of MFR can simultaneously inhibit osteoclast and osteoblast differentiation. These results may be related to the insignificant effect of the MFR-H group compared to the MFR-L in bone loss in the OVX-induced rat model.

In conclusion, the effects of MFR on RANKL-induced osteoclast differentiation and ovariectomy-induced bone loss in a SD-rat model were determined. *In vitro*, MFR reduced RANKL-induced osteoclast differentiation, function and formation. MFR downregulated the expression levels of master transcription factors, such as NFATc1 and c-Fos. In addition, MFR reduced the expression levels of MMP-9, CTK, CA2, TRAP, ATP6v0d2, DC-STAMP, OSCAR, c-Src and Blimp-1 through the downregulation of NFATc1 and c-Fos signaling. *In vivo*, MFR-L increased BMD in the OVX-induced bone loss model. MFR-H exhibited insignificant effects on the OVX-induced bone loss model compared with MFR-L.

The present study had several limitations, as follows: i) *In vitro*, MFR inhibited RANKL-induced expression of NFATc1 and c-Fos signaling. MAPK and NF-κB signaling pathways are also involved in NFATc1 and c-Fos signaling; however, the effect of MFR was not determined on these factors. To further assess the mechanisms underlying the inhibitory effects of MFR on osteoclast differentiation via the NFATc1 and c-Fos pathway, further studies regarding the involvement of MAPKs and NF-κB are required. ii) When comparing the pharmacological effects of MFR in the *in vitro* experiments and *in vivo* experiments, MFR showed a relatively low pharmacological effect in *in vivo* experiments compared with that in the *in vitro* experiments. Therefore, further research on the effects of MFR on osteoclast-mediated bone diseases, such as in the LPS-induced bone loss model, senile osteoporosis and osteoporosis caused by steroid side effects, are necessary. iii) In the micro-CT test results, MFR-L increased BMD; however, it did not significantly affect the bone micro-architecture. In general, an increase in BMD is associated with changes in the bone micro-architecture;

however, this is not the case in this study. Further studies are required to determine the reason behind this. iv) The present study focused on the effects of MFR on inhibition of osteoclast differentiation; According to previous studies, MFR contains a variety of components (85), and constituents of MFR, such as vitexin, linarin, ecdysterone and ursolic acid, were found to be effective in inhibiting osteoclast differentiation. Vitexin inhibited osteoclast differentiation and osteolysis (28), and Wang *et al* (84) revealed the inhibitory activity of linarin on osteoclastogenesis through the RANKL-induced NF-κB pathway. In addition, ecdysterone, another active compound in MFR, prevented LPS-induced osteoclastogenesis (86). Ursolic acid has also been shown to inhibit osteoclastogenesis and titanium particle-induced osteolysis (87). However, to the best of our knowledge, the effects of most of the components of MFR on osteoclast differentiation have not been studied. Therefore, analyzing the effect of each component of MFR on osteoclast differentiation will help to understand the underlying anti-osteoporotic mechanism of MFR.

Acknowledgements

Not applicable.

Funding

This work was supported by the National Research Foundation of Korea grant funded by the Korean government (grant nos. 2019R1H1A2101224 and 2020R1A2C1007836).

Availability of data and materials

All data generated or analyzed during this study are included in this published article.

Authors' contributions

YS designed the study. MK and BK prepared the extract. MK, JHK and EYK performed the *in vitro* experiments and analyzed the data. MK, JHK, SH and BK performed the *in vivo* experiments and analyzed the data. MK, JHK and HSI contributed to the statistical analysis and helped interpret the results. YS supervised the experiments in discussion with JHK and MK. MK and JHK wrote the manuscript. MK and JHK confirm the authenticity of all the raw data. All authors read and approved the final manuscript.

Ethics approval and consent to participate

The protocols for this experiment were approved by the Kyung Hee Medical Science Research Institute Animal Care and Use Committee (approval no. KHMC-IACUC 19-017).

Patient consent for publication

Not applicable.

Competing interests

The authors declare that they have no competing interests.

References

- Matsuo K and Irie N: Osteoclast-osteoblast communication. *Arch Biochem Biophys* 473: 201-209, 2008.
- Riggs BL and Melton LJ III: The worldwide problem of osteoporosis: Insights afforded by epidemiology. *Bone* 17 (Suppl 5): 505S-511S, 1995.
- Sözen T, Özışık L and Başaran NÇ: An overview and management of osteoporosis. *Eur J Rheumatol* 4: 46-56, 2017.
- Feng X and McDonald JM: Disorders of bone remodeling. *Annu Rev Pathol* 6: 121-145, 2011.
- Tella SH and Gallagher JC: Prevention and treatment of postmenopausal osteoporosis. *J Steroid Biochem Mol Biol* 142: 155-170, 2014.
- Khosla S, Burr D, Cauley J, Dempster DW, Ebeling PR, Felsenberg D, Gagel RF, Gilsanz V, Guise T, Koka S, *et al.*: Bisphosphonate-associated osteonecrosis of the jaw: Report of a task force of the American society for bone and mineral research. *J Bone Miner Res* 22: 1479-1491, 2007.
- Wysowski DK: Reports of esophageal cancer with oral bisphosphonate use. *N Engl J Med* 360: 89-90, 2009.
- Kennel KA and Drake MT: Adverse effects of bisphosphonates: Implications for osteoporosis management. *Mayo Clin Proc* 84: 632-638, 2009.
- Lenart BA, Lorch DG and Lane JM: Atypical fractures of the femoral diaphysis in postmenopausal women taking alendronate. *N Engl J Med* 358: 1304-1306, 2008.
- Manson JE, Hsia J, Johnson KC, Rossouw JE, Assaf AR, Lasser NL, Trevisan M, Black HR, Heckbert SR, Detrano R, *et al.*: Estrogen plus progestin and the risk of coronary heart disease. *N Engl J Med* 349: 523-534, 2003.
- Collaborative Group On Epidemiological Studies Of Ovarian Cancer, Beral V, Gaitskell K, Hermon C, Moser K, Reeves G and Peto R: Menopausal hormone use and ovarian cancer risk: Individual participant meta-analysis of 52 epidemiological studies. *Lancet* 385: 1835-1842, 2015.
- Puhalla S, Bhattacharya S and Davidson NE: Hormonal therapy in breast cancer: A model disease for the personalization of cancer care. *Mol Oncol* 6: 222-236, 2012.
- Collin-Osdoby P, Yu X, Zheng H and Osdoby P: RANKL-mediated osteoclast formation from murine RAW 264.7 cells. *Methods Mol Biol* 80: 153-166, 2003.
- Suda T, Takahashi N, Udagawa N, Jimi E, Gillespie MT and Martin TJ: Modulation of osteoclast differentiation and function by the new members of the tumor necrosis factor receptor and ligand families. *Endocr Rev* 20: 345-357, 1999.
- Ye H, Arron JR, Lamothe B, Cirilli M, Kobayashi T, Shevde NK, Segal D, Dzivenu OK, Vologodskaja M, Yim M, *et al.*: Distinct molecular mechanism for initiating TRAF6 signalling. *Nature* 418: 443-447, 2002.
- Galibert L, Tometsko ME, Anderson DM, Cosman D and Dougall WC: The involvement of multiple tumor necrosis factor receptor (TNFR)-associated factors in the signaling mechanisms of receptor activator of NF- κ B, a member of the TNFR superfamily. *J Biol Chem* 273: 34120-34127, 1998.
- Roy A, Kim YB, Cho KH and Kim JH: Glucose starvation-induced turnover of the yeast glucose transporter Hxt1. *Biochim Biophys Acta* 1840: 2878-2885, 2014.
- Boyle WJ, Simonet WS and Lacey DL: Osteoclast differentiation and activation. *Nature* 423: 337-342, 2003.
- Takayanagi H, Kim S, Koga T, Nishina H, Isshiki M, Yoshida H, Saiura A, Isobe M, Yokochi T, Inoue J, *et al.*: Induction and activation of the transcription factor NFATc1 (NFAT2) integrate RANKL signaling in terminal differentiation of osteoclasts. *Dev Cell* 3: 889-901, 2002.
- Arai A, Mizoguchi T, Harada S, Kobayashi Y, Nakamichi Y, Yasuda H, Penninger JM, Yamada K, Udagawa N and Takahashi N: Fos plays an essential role in the upregulation of RANK expression in osteoclast precursors within the bone microenvironment. *J Cell Sci* 125: 2910-2917, 2012.
- Perry LM and Metzger J: Medicinal plants of east and southeast Asia: Attributed properties and uses. Cambridge: MIT Press, 1980.
- Jeong YH, Oh YC, Cho WK, Lee B and Ma JY: Anti-inflammatory effects of melandrii herba ethanol extract via inhibition of NF- κ B and MAPK signaling pathways and induction of HO-1 in RAW 264.7 cells and mouse primary macrophages. *Molecules* 21: 818, 2016.
- Herbology editorial committee of Korean medicine schools. Herbology. Seoul: Yeonglimsa, pp306-308, 2012.
- Redlich K and Smolen JS: Inflammatory bone loss: Pathogenesis and therapeutic intervention. *Nat Rev Drug Discov* 11: 234-250, 2012.
- Lacativa PG and Farias ML: Osteoporosis and inflammation. *Arq Bras Endocrinol Metabol* 54: 123-132, 2010.
- McLean RR: Proinflammatory cytokines and osteoporosis. *Curr Osteoporos Rep* 7: 134-139, 2009.
- Ruscitti P, Cipriani P, Carubbi F, Liakouli V, Zazzeroni F, Di Benedetto P, Berardicurti O, Alesse E and Giacomelli R: The role of IL-1 β in the bone loss during rheumatic diseases. *Mediators Inflamm* 2015: 782382, 2015.
- Jiang J, Jia Y, Lu X, Zhang T, Zhao K, Fu Z, Pang C and Qian Y: Vitexin suppresses RANKL-induced osteoclastogenesis and prevents lipopolysaccharide (LPS)-induced osteolysis. *J Cell Physiol* 234: 17549-17560, 2019.
- Lee MY, Shin IS, Seo CS, Lee NH, Ha HK, Son JK and Shin HK: Effects of *Melandrium firmum* methanolic extract on testosterone-induced benign prostatic hyperplasia in Wistar rats. *Asian J Androl* 14: 320-324, 2012.
- Taciak B, Bialasek M, Braniewska A, Sas Z, Sawicka P, Kiraga Ł, Rygiel T and Król M: Evaluation of phenotypic and functional stability of RAW 264.7 cell line through serial passages. *PLoS One* 13: e0198943, 2018.
- Ballanti P, Minisola S, Pacitti MT, Scarnecchia L, Rosso R, Mazzuoli GF and Bonucci E: Tartrate-resistant acid phosphatase activity as osteoclastic marker: Sensitivity of cytochemical assessment and serum assay in comparison with standardized osteoclast histomorphometry. *Osteoporos Int* 7: 39-43, 1997.
- Tschöp MH, Speakman JR, Arch JR, Auwerx J, Brüning JC, Chan L, Eckel RH, Farese RV Jr, Galgani JE, Hambly C, *et al.*: A guide to analysis of mouse energy metabolism. *Nat Methods* 9: 57-63, 2011.
- Kim JH, Kim M, Jung HS and Sohn Y: Leonurus sibiricus L. ethanol extract promotes osteoblast differentiation and inhibits osteoclast formation. *Int J Mol Med* 44: 913-926, 2019.
- Kim M, Kim M, Kim JH, Hong S, Kim DH, Kim S, Kim EY, Jung HS and Sohn Y: Crataegus pinnatifida bunge inhibits RANKL-induced osteoclast differentiation in RAW 264.7 cells and prevents bone loss in an ovariectomized rat model. *Evid Based Complement Alternat Med* 2021: 5521562, 2021.
- Beconi MG, Howland D, Park L, Lyons K, Giuliano J, Dominguez C, Munoz-Sanjuan I and Pacifici R: Pharmacokinetics of memantine in rats and mice. *PLoS Curr* 3: RRN1291, 2011.
- Jurđić P, Saltel F, Chabadel A and Destaing O: Podosome and sealing zone: Specificity of the osteoclast model. *Eur J Cell Biol* 85: 195-202, 2006.
- Zhao Q, Wang X, Liu Y, He A and Jia R: NFATc1: Functions in osteoclasts. *Int J Biochem Cell Biol* 42: 576-579, 2010.
- Grigoriadis AE, Wang ZQ, Cecchini MG, Hofstetter W, Felix R, Fleisch HA and Wagner EF: c-Fos: A key regulator of osteoclast-macrophage lineage determination and bone remodeling. *Science* 266: 443-448, 1994.
- Kim K, Lee SH, Ha Kim J, Choi Y and Kim N: NFATc1 induces osteoclast fusion via up-regulation of Atp6v0d2 and the dendritic cell-specific transmembrane protein (DC-STAMP). *Mol Endocrinol* 22: 176-185, 2008.
- Sharp PE, La Regina MC and Suckow MA: The laboratory rat. Boca Raton, CRC Press, 1998.
- Hansan KMM, Tamanna N and Haque MA: Biochemical and histopathological profiling of Wistar rat treated with Brassica napus as a supplementary feed. *Food Sci Hum Well* 7: 77-82, 2018.
- Sudo H, Kodama HA, Amagai Y, Yamamoto S and Kasai S: In vitro differentiation and calcification in a new clonal osteogenic cell line derived from newborn mouse calvaria. *J Cell Biol* 96: 191-198, 1983.
- Gregory CA, Gunn WG, Peister A and Prockop DJ: An Alizarin red-based assay of mineralization by adherent cells in culture: Comparison with cetylpyridinium chloride extraction. *Anal Biochem* 329: 77-84, 2004.
- Hartley JW, Evans LH, Green KY, Naghashfar Z, Macias AR, Zervas PM and Ward JM: Expression of infectious murine leukemia viruses by RAW264.7 cells, a potential complication for studies with a widely used mouse macrophage cell line. *Retrovirology* 5: 1, 2008.
- Collin-Osdoby P and Osdoby P: RANKL-mediated osteoclast formation from murine RAW 264.7 cells. *Methods Mol Biol* 816: 187-202, 2012.
- Kirstein B, Chambers TJ and Fuller K: Secretion of tartrate-resistant acid phosphatase by osteoclasts correlates with resorptive behavior. *J Cell Biochem* 98: 1085-1094, 2006.
- Hayman AR: Tartrate-resistant acid phosphatase (TRAP) and the osteoclast/immune cell dichotomy. *Autoimmunity* 41: 218-223, 2008.

48. Marchisio PC, Cirillo D, Naldini L, Primavera MV, Teti A and Zamboni-Zallone A: Cell-substratum interaction of cultured avian osteoclasts is mediated by specific adhesion structures. *J Cell Biol* 99: 1696-1705, 1984.
49. Hsu H, Lacey DL, Dunstan CR, Solovyev I, Colombero A, Timms E, Tan HL, Elliott G, Kelley MJ, Sarosi I, *et al*: Tumor necrosis factor receptor family member RANK mediates osteoclast differentiation and activation induced by osteoprotegerin ligand. *Proc Natl Acad Sci USA* 96: 3540-3545, 1999.
50. Jimi E, Akiyama S, Tsurukai T, Okahashi N, Kobayashi K, Udagawa N, Nishihara T, Takahashi N and Suda T: Osteoclast differentiation factor acts as a multifunctional regulator in murine osteoclast differentiation and function. *J Immunol* 163: 434-442, 1999.
51. Naito A, Azuma S, Tanaka S, Miyazaki T, Takaki S, Takatsu K, Nakao K, Nakamura K, Katsuki M, Yamamoto T and Inoue J: Severe osteopetrosis, defective interleukin-1 signalling and lymph node organogenesis in TRAF6-deficient mice. *Genes Cells* 4: 353-362, 1999.
52. Wong BR, Josien R, Lee SY, Vologodskiaia M, Steinman RM and Choi Y: The TRAF family of signal transducers mediates NF-kappaB activation by the TRANCE receptor. *J Biol Chem* 273: 28355-28359, 1998.
53. Hayden MS and Ghosh S: Shared principles in NF-kappaB signaling. *Cell* 132: 344-362, 2008.
54. Yamashita T, Yao Z, Li F, Zhang Q, Badell IR, Schwarz EM, Takeshita S, Wagner EF, Noda M, Matsuo K, *et al*: NF-kappaB p50 and p52 regulate receptor activator of NF-kappaB ligand (RANKL) and tumor necrosis factor-induced osteoclast precursor differentiation by activating c-Fos and NFATc1. *J Biol Chem* 282: 18245-18253, 2007.
55. Ray N, Kuwahara M, Takada Y, Maruyama K, Kawaguchi T, Tsubone H, Ishikawa H and Matsuo K: c-Fos suppresses systemic inflammatory response to endotoxin. *Int Immunol* 18: 671-677, 2006.
56. Fujioka S, Niu J, Schmidt C, Sclabas GM, Peng B, Uwagawa T, Li Z, Evans DB, Abbruzzese JL and Chiao PJ: NF-kappaB and AP-1 connection: Mechanism of NF-kappaB-dependent regulation of AP-1 activity. *Mol Cell Biol* 24: 7806-7819, 2004.
57. Landström M: The TAK1-TRAF6 signalling pathway. *Int J Biochem Cell Biol* 42: 585-589, 2010.
58. Wei ZF, Tong B, Xia YF, Lu Q, Chou GX, Wang ZT and Dai Y: Norisoboldine suppresses osteoclast differentiation through preventing the accumulation of TRAF6-TAK1 complexes and activation of MAPKs/NF-κB/c-Fos/NFATc1 pathways. *PLoS One* 8: e59171, 2013.
59. Sundaram K, Nishimura R, Senn J, Youssef RF, London SD and Reddy SV: RANK ligand signaling modulates the matrix metalloproteinase-9 gene expression during osteoclast differentiation. *Exp Cell Res* 313: 168-178, 2007.
60. Troen BR: The role of cathepsin K in normal bone resorption. *Drug News Perspect* 17: 19-28, 2004.
61. David JP, Rincon M, Neff L, Horne WC and Baron R: Carbonic anhydrase II is an AP-1 target gene in osteoclasts. *J Cell Physiol* 188: 89-97, 2001.
62. Yagi M, Miyamoto T, Sawatani Y, Iwamoto K, Hosogane N, Fujita N, Morita K, Ninomiya K, Suzuki T, Miyamoto K, *et al*: DC-STAMP is essential for cell-cell fusion in osteoclasts and foreign body giant cells. *J Exp Med* 202: 345-351, 2005.
63. Lee SH, Rho J, Jeong D, Sul JY, Kim T, Kim N, Kang JS, Miyamoto T, Suda T, Lee SK, *et al*: v-ATPase V0 subunit d2-deficient mice exhibit impaired osteoclast fusion and increased bone formation. *Nat Med* 12: 1403-1409, 2006.
64. Kim JH, Kim K, Jin HM, Youn BU, Song I, Choi HS and Kim N: Upstream stimulatory factors regulate OSCAR gene expression in RANKL-mediated osteoclast differentiation. *J Mol Biol* 383: 502-511, 2008.
65. Miyazaki T, Tanaka S, Sanjay A and Baron R: The role of c-Src kinase in the regulation of osteoclast function. *Mod Rheumatol* 16: 68-74, 2006.
66. Nishikawa K, Nakashima T, Hayashi M, Fukunaga T, Kato S, Kodama T, Takahashi S, Calame K and Takayanagi H: Blimp1-mediated repression of negative regulators is required for osteoclast differentiation. *Proc Natl Acad Sci USA* 107: 3117-3122, 2010.
67. Miyauchi Y, Ninomiya K, Miyamoto H, Sakamoto A, Iwasaki R, Hoshi H, Miyamoto K, Hao W, Yoshida S, Morioka H, *et al*: The Blimp1-Bcl6 axis is critical to regulate osteoclast differentiation and bone homeostasis. *J Exp Med* 207: 751-762, 2010.
68. Eastell R, O'Neill TW, Hofbauer LC, Langdahl B, Reid IR, Gold DT and Cummings SR: Postmenopausal osteoporosis. *Nat Rev Dis Primers* 2: 16069, 2016.
69. Riggs BL, Khosla S and Melton LJ III: A unitary model for involutional osteoporosis: Estrogen deficiency causes both type I and II osteoporosis in postmenopausal women and contributes to bone loss in aging men. *J Bone Miner Res* 13: 763-773, 1998.
70. Kalu DN: The ovariectomized rat model of postmenopausal bone loss. *Bone Miner* 15: 175-191, 1991.
71. Kuo TR and Chen CH: Bone biomarker for the clinical assessment of osteoporosis: Recent developments and future perspectives. *Biomark Res* 5: 18, 2017.
72. Wu X, Xie CQ, Zhu QQ, Wang MY, Sun B, Huang YP, Shen C, An MF, Zhao YL, Wang XJ and Sheng J: Green tea (*Camellia sinensis*) aqueous extract alleviates postmenopausal osteoporosis in ovariectomized rats and prevents RANKL-induced osteoclastogenesis in vitro. *Food Nutr Res* 62, 2018.
73. Ozer J, Ratner M, Shaw M, Bailey W and Schomaker S: The current state of serum biomarkers of hepatotoxicity. *Toxicology* 245: 194-205, 2008.
74. Wronski TJ, Cintrón M and Dann LM: Temporal relationship between bone loss and increased bone turnover in ovariectomized rats. *Calcif Tissue Int* 43: 179-183, 1988.
75. Ito M: Recent progress in bone imaging for osteoporosis research. *J Bone Miner Metab* 29: 131-140, 2011.
76. Bouxsein ML, Boyd SK, Christiansen BA, Guldberg RE, Jepsen KJ and Müller R: Guidelines for assessment of bone microstructure in rodents using micro-computed tomography. *J Bone Miner Res* 25: 1468-1486, 2010.
77. Park SB, Lee YJ and Chung CK: Bone mineral density changes after ovariectomy in rats as an osteopenic model: Stepwise description of double dorso-lateral approach. *J Korean Neurosurg Soc* 48: 309-312, 2010.
78. Parkinson IH and Fazzalari NL: Interrelationships between structural parameters of cancellous bone reveal accelerated structural change at low bone volume. *J Bone Miner Res* 18: 2200-2205, 2003.
79. Osterhoff G, Morgan EF, Shefelbine SJ, Karim L, McNamara LM and Augat P: Bone mechanical properties and changes with osteoporosis. *Injury* 47 (Suppl 2): S11-S20, 2016.
80. Kim EY, Kim JH, Kim M, Park JH, Sohn Y and Jung HS: Abeliophyllum distichum Nakai alleviates postmenopausal osteoporosis in ovariectomized rats and prevents RANKL-induced osteoclastogenesis in vitro. *J Ethnopharmacol* 257: 112828, 2020.
81. Lee KY, Kim JH, Kim EY, Yeom M, Jung HS and Sohn Y: Water extract of *Cnidii Rhizoma* suppresses RANKL-induced osteoclastogenesis in RAW 264.7 cell by inhibiting NFATc1/c-Fos signaling and prevents ovariectomized bone loss in SD-rat. *BMC Complement Altern Med* 19: 207, 2019.
82. Kim M, Kim HS, Kim JH, Kim EY, Lee B, Lee SY, Jun JY, Kim MB, Sohn Y and Jung HS: Chaenomelis fructus inhibits osteoclast differentiation by suppressing NFATc1 expression and prevents ovariectomy-induced osteoporosis. *BMC Complement Med Ther* 20: 35, 2020.
83. Kim JH, Kim EY, Lee B, Min JH, Song DU, Lim JM, Eom JW, Yeom M, Jung HS and Sohn Y: The effects of lycii radicis cortex on RANKL-induced osteoclast differentiation and activation in RAW 264.7 cells. *Int J Mol Med* 37: 649-658, 2016.
84. Wang J, Fu B, Lu F, Hu X, Tang J and Huang L: Inhibitory activity of linarin on osteoclastogenesis through receptor activator of nuclear factor kappaB ligand-induced NF-kappaB pathway. *Biochem Biophys Res Commun* 495: 2133-2138, 2018.
85. Seo CS and Shin HK: Simultaneous determination of the five marker compounds in melandriumfirmum using high-performance liquid chromatography with photodiode-array detection. *Nat Prod Commun* 11: 1667-1669, 2016.
86. Li Y, Zhang J, Yan C, Chen Q, Xiang C, Zhang Q, Wang X and Jiang K: β-Ecdysterone prevents LPS-induced osteoclastogenesis by regulating NF-κB pathway in vitro. *Res Square*, 2020.
87. Jiang C, Xiao F, Gu X, Zhai Z, Liu X, Wang W, Tang T, Wang Y, Zhu Z, Dai K, *et al*: Inhibitory effects of ursolic acid on osteoclastogenesis and titanium particle-induced osteolysis are mediated primarily via suppression of NF-κB signaling. *Biochimie* 111: 107-118, 2015.

